Final Report

DEVELOPMENT AND DEMONSTRATION OF ENERGY–CONSERVING DRYING MODIFICATIONS TO TEXTILE PROCESSES

Investigators:

D. S. Brookstein
W. W. Carr
W. D. Holcombe

Prepared for

U. S. DEPARTMENT OF ENERGY
ASSISTANT SECRETARY FOR CONSERVATION
AND SOLAR ENERGY
OFFICE OF INDUSTRIAL PROGRAMS

GEORGIA INSTITUTE OF TECHNOLOGY
SCHOOL OF TEXTILE ENGINEERING
ATLANTA, GEORGIA 30332

1980

DOE Form IR-426
(1/79)

U.S. DEPARTMENT OF ENERGY

DOE AND MAJOR CONTRACTOR RECOMMENDATIONS FOR DISPOSITION OF SCIENTIFIC AND TECHNICAL DOCUMENT

See Instructions on Reverse Side

1. DOE Report No.	2. Contract No.	3. Subject Category No.
	DE-AS05-76CS40081	

4. Title: Development and Demonstration of Energy Conserving Drying Modifications to Textile Processes

5. Type of Document ("x" one)
- ☒ a. Scientific and technical report
- ☐ b. Conference paper: Title of conference _____

_____ Date of conference _____

Exact location of conference _____ Sponsoring organization _____

- ☐ c. Other (Specify Thesis, Translations, etc.)

6. Copies Transmitted ("x" one or more)
- ☒ a. Copies being transmitted for standard distribution by DOE–TIC.
- ☐ b. Copies being transmitted for special distribution per attached complete address list.
- ☐ c. Two completely legible, reproducible copies being transmitted to DOE–TIC.
- ☐ d. Twenty-seven copies being transmitted to DOE–TIC for TIC processing and NTIS sales.

7. Recommended Distribution ("x" one)
- ☒ a. Normal handling (after patent clearance): no restraints on distribution except as may be required by the security classification.

Make available only ☐ b. to U.S. Government agencies and their contractors. ☐ c. within DOE and to DOE contractors. ☐ d. within DOE. ☐ e. to those listed in item 13 below.

- ☒ f. Other (Specify) Textile Industry Trade Organizations

8. Recommended Announcement ("x" one)
- ☒ a. Normal procedure may be followed. ☐ b. Recommend the following announcement limitations:

9. Reason for Restrictions Recommended in 7 or 8 above.
- ☐ a. Preliminary information. ☐ b. Prepared primarily for internal use. ☐ c. Other (Explain)

10. Patent Clearance

Does this information product disclose any new equipment, process or material? ☐ Yes ☒ No

Has an invention disclosure been submitted to DOE covering any aspect of this information product? If so, identify the DOE (or other) disclosure number and to whom the disclosure was submitted. ☐ Yes ☒ No

Are there any patent related objections to the release of this information product? If so, state these objections.

No

("x" one)
- ☐ a. DOE patent clearance has been granted by responsible DOE patent group.
- ☐ b. Document has been sent to responsible DOE patent group for clearance.

11. National Security Information (For classified document only; "x" one)

Document ☐ a. does ☒ b. does not contain national security information other than restricted data.

12. Copy Reproduction and Distribution

Total number of copies reproduced _____ Number of copies distributed outside originating organization _____

13. Additional Information or Remarks (Continue on separate sheet, if necessary)

14. Submitted by (Name and Position) (Please print or type)

Dr. Wallace W. Carr, Associate Professor

Organization

School of Textile Engineering, Georgia Institute of Technology

Signature	Date
[redacted]	08-11-80

DEVELOPMENT AND DEMONSTRATION OF ENERGY-CONSERVING DRYING MODIFICATIONS TO TEXTILE PROCESSES

Final Report

Part II, Phase III Extension of
DOE Contract No. DE-AS05-76CS40081

Modification No. M004

Prepared By

School of Textile Engineering

and

Engineering Experiment Station

of

THE GEORGIA INSTITUTE OF TECHNOLOGY
Atlanta, Georgia 30332

Investigators:

D. S. Brookstein
W. W. Carr
W. D. Holcombe

Prepared For:

U.S. Department of Energy
Assistant Secretary for Conservation
and Solar Energy
Office of Industrial Programs

DEVELOPMENT AND DEMONSTRATION OF ENERGY-CONSERVING DRYING MODIFICATIONS TO TEXTILE PROCESSES

Final Report

Part II, Phase III Extension of
DOE Contract No. DE-AS05-76CS40081

Modification No. M004

Covering the Period

December 1, 1978 - November 30, 1979

Prepared by

The School of Textile Engineering

and

The Engineering Experiment Station

of

THE GEORGIA INSTITUTE OF TECHNOLOGY
Atlanta, Georgia 30332

Principal Investigator:
Dr. D. S. Brookstein
Assistant Professor

Senior Engineer:
Dr. W. W. Carr
Associate Professor

Research Engineer:
Mr. W. D. Holcome

Graduate Research Assistant:
Mr. A. Mahadevan

Prepared for:

U.S. Department of Energy
Assistant Secretary for Conservation
and Solar Energy
Office of Industrial Programs

TABLE OF CONTENTS

ACKNOWLEDGMENTS

The authors gratefully acknowledge the support extended to the project by the textile industry. Advice, guidance, and materials were freely given.

Special appreciation is due to the DOE Technical Monitor for the project, Mr. John Rossmeissl, for his valuable guidance and support. The authors are also grateful to Mr. Al Streb and Mr. Doug Harvey of DOE for the Administrative roles in the project.

Special appreciation is also due to Dr. W. C. Tincher, Acting Director of the School of Textile Engineering, who suggested that the Machnozzle be investigated as a fabric predrying device.

Special thanks are due to Dr. M. V. Konopasek for his time and assistance in setting up the computational scheme. The authors would like to extend a special word of appreciation to Professor W. F. Ames for his time and advice on the numerical scheme.

LIST OF TABLES

LIST OF FIGURES

LIST OF FIGURES (cont'd.)

LIST OF APPENDICES

SUMMARY

Textile drying processes are very energy extensive, consuming approximately 24% of the energy used in wet processing of textiles. The purpose of the work under this research program was to develop and to expand procedural and engineering modifications to textile drying processes in order to reduce energy requirements. Research was concentrated in two major areas: 1) an investigation of the potential of a Machnozzle as a fabric predrying device and 2) a program to optimize textile can drying with respect to energy consumption.

Tests were run to evaluate the Machnozzle as a predrying device to be used just prior to final drying. Three types of fabric (100% cotton, 50/50 polyester/cotton, and 100% polyester) were tested. The test results clearly demonstrated that the Machnozzle can significantly reduce the moisture content in fabric. The Machnozzle reduced the moisture content of 100% cotton fabrics weighing 4.0 oz/yd^2 from approximately 97% to 34 and 46% for fabric speeds of 20 and 80 m/min, respectively. The moisture content of 50/50 cotton/polyester fabrics weighing 3.6 oz/yd^2 was reduced from 68% to 7 and 17% for fabric speeds of 20 and 80 m/min, respectively. The Machnozzle was extremely effective in removing moisture from 100% polyester fabric weighing 1.8 oz/yd^2. The moisture content was reduced from approximately 61% to 3 and 6% for fabric speeds of 20 and 80 m/min, respectively.

The energy consumption of the Machnozzle compares favorably with that for steam can dryers. Typically, steam can dryers require between 1.5 and 2.0 pounds of steam per pound of water removed. The Machnozzle consumes approxi-

mately 1.0 pound of steam per pound of water removed when processing all three types of fabrics at 80 m/min (which corresponds closely with industrial process speeds). When the energy recovered by the condenser system is considered, the Machnozzle becomes even more attractive as a fabric predrying device. With recovery, the steam consumption of the Machnozzle is approximately 0.3 pound of steam per pound of water removed.

An economic analysis of the Machnozzle as a predrying device was made. The parameter used to judge the economic performance of the Machnozzle was Internal Rate of Return (IRR). The results of the calculations showed that the economic feasibility of using the Machnozzle as a predrying device depends on the cost of energy and process operating conditions. Internal Rate of Return (IRR) was very large (as high as 183%) in some cases, but extremely small in other cases. For some operating conditions (lower fabric speeds), the initial investment would not be recovered in the ten year period used in the analysis.

An Internal Rate of Return (IRR) of 50% is usually considered the lower limit of economically feasible energy-conservation investments in the textile industry. With this constraint on Internal Rate of Return (IRR) and an energy cost of $3 per million BTU, the economic analysis indicates that the Machnozzle is attractive for 100% cotton fabrics and 50/50 cotton/polyester blend fabrics processed at 80 m/min. All three types of fabrics give favorable Internal Rate of Return (IRR) at an energy cost of $3 per million BTU plus 10% per year.

The use of steam cans for drying is prevalent in the textile industry. Due to the low cost of energy in the past, low energy consumption has not been a criterion in the design and operation of steam cans. As a result, steam cans are energy inefficient in the drying of textiles. Since textile can

drying represents an energy-intensive, wasteful process, one of the objectives of this research was to reduce the energy required in textile can drying. An experimental approach to optimize steam can drying with respect to energy consumption is a very tedious and expensive process. Accordingly, a mathematical model describing the physical aspects of the can drying process has been developed to predict drying rates. A numerical scheme for the solution of the governing equations is presented. Due to the lack of available data on drying of textiles, the results were compared with experimental data for paper drying. Comparable temperature-time and moisture content-time profiles were obtained. The importance of critical heat and mass transfer parameters is discussed.

I. INTRODUCTION

Data collected in Phase I of DOE Contract Number EY-76-S-05-5099, "Energy Conservation in the Textile Industry", revealed that predrying and drying of textiles consumes approximately 8.8×10^6 barrels of oil equivalent energy annually or approximately 24% of the total energy consumed in wet processing of textiles(1). Predrying and drying processes have relied heavily on thermal energy to remove water and have been energy inefficient. Therefore, predrying and drying were targeted as processes where research and development in Phase II of the DOE project could lead to significant energy conservation.

During Phase II (2) of the DOE project, methods for combining mechanical and thermal means of moisture removal were investigated. One of the moisture removal techniques involved the use of a novel drying device called a Machnozzle. The Machnozzle is designed to accelerate high pressure steam to sonic speed by passing it through a narrow slot. The fabric is passed across the slot exit where the high velocity steam flow creates a large pressure differential across the fabric. The water is then literally blown out of the fabric. The steam passing through the fabric loses little of its thermal energy and can therefore be mixed with cold water to yield a hot water source for the plant.

The major role of the Georgia Tech research on the Machnozzle was to evaluate and optimize the device while comparing the drying efficiency to the manufacturer's claims. A 16-inch long Machnozzle was purchased, and a test system was built which simulated projected plant conditions of fabric speed and steam pressures. Due to project limitations, no runs were possible on the unit before Phase II termination.

Additional funding was granted to Georgia Tech to conduct the drying research reported herein. The purpose of the research was to demonstrate further and to expand procedural and engineering modifications to textile drying processes in order to reduce energy requirements. The modifications were approached cognizant of the requirement of maintaining or improving existing process production efficiency and product quality. Specific objectives of the research were:

1. To develop further and to expand energy-conserving procedural and engineering modifications to textile drying process, in particular, to investigate the potential of the Machnozzle as a predrying device.

2. To demonstrate the developed modifications on a pilot-scale basis.

3. To derive energy savings based on the pilot-scale data and conventional textile process data.

4. To examine cost/benefit relationships of the demonstrated modifications and determine the feasibility of technology transfer to participating plants.

5. To disseminate the results of the research to the industry through short courses, workshops, trade publications and organizations, and relevant Georgia Tech courses.

The research to accomplish these objectives was concentrated in two major areas:

1. An investigation of the potential of a Machnozzle as a fabric predrying device.

2. A program to optimize textile can drying with respect to energy consumption.

II. PILOT-SCALE STUDIES OF A MACHNOZZLE AS A PREDRYING DEVICE

A. BACKGROUND

Textile drying is an energy-intensive process consuming approximately 8.8×10^6 barrels-of-oil equivalent energy annually or approximately 24% of the total energy consumed in wet processing of textiles(1). Drying processes have relied heavily on thermal energy to remove water and have been energy inefficient. During Phase I of DOE Contract Number EY-76-S-05-5099, "Energy Conservation in the Textile Industry", predrying and drying processes were identified as processes where research and development in Phase II of the DOE project could lead to significant energy conservation.

Methods for combining mechanical and thermal means of moisture removal were investigated during Phase II of the DOE project. One of the moisture removal techniques involved the use of a novel drying device called a Machnozzle. A 16-inch long Machnozzle was purchased, and a test system was built which simulated projected plant conditions of fabric speed and steam pressures. Due to project limiations, no runs were possible on the unit before Phase II termination.

Additional funding was granted to Georgia Tech to conduct the drying research discussed in this report. The major part of the research effort was directed at evaluating the Machnozzle as a predrying device to be used just to final drying.

Brugman Machinefabrik of the Netherlands developed the Machnozzle as a moisture removal device to be used in conjunction with washers manufactured by Burgman Machinefabrik. Claims made by Burgman Machinefabrik indicated that the Machnozzle could significantly decrease the moisture content in fabrics and had

a potential for reducing energy consumed in drying textiles(3,4). The claims suggested that the Machnozzle is capable of drying fabrics to lower moisture levels than may be obtained with other mechanical extraction systems such as pressure rolls, while having a much lower energy consumption than is required in thermal drying. However, problems were encountered with the application of the Machnozzle in the washer systems due to lint build up on the Machnozzle and dyeing nonuniformity.

The problems associated with the application of the Machnozzle in the washer systems should not be encountered when the Machnozzle is used as separate unit functioning as a predrying device just prior to final drying. If used in this manner, the Machnozzle could reduce the amount of moisture that must be evaporated in the energy intensive final drying stage. Thus tests were conducted at Georgia Tech to evaluate the Machnozzle as a predrying device.

B. DESCRIPTION OF THE MACHNOZZLE

A cross section of the Machnozzle apparatus is shown in Figure 1. Steam or some other gas if fed by a pipeline to the Machnozzle. The steam flows at very low speed through most of the Machnozzle until it reaches a buffer chamber (the circular chamber located near the tip of the Machnozzle). As the steam leaves the chamber, it accelerates rapidly as it moves through a converging nozzle and then through a very narrow slot (0.001-inch wide). At the exit of the nozzle, the steam velocity is sonic if the input steam pressure is sufficiently high. When fabric is passed across the exit of the slot, the high velocity steam flow creates a large pressure differential across the fabric. Water and residual matter entrained around and in the yarn are literally blown out of the fabric, with little heat transfer occurring. The steam passing

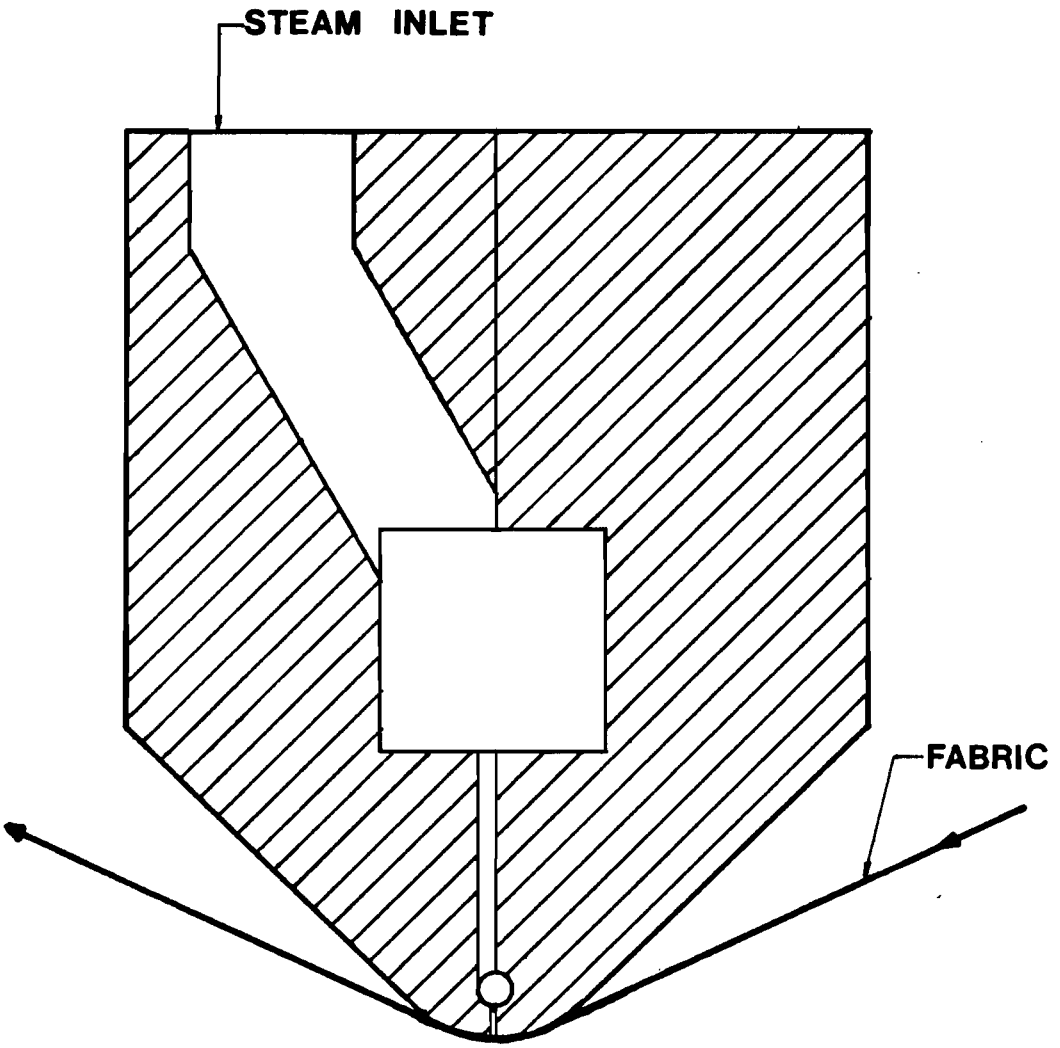

Figure 1. Cross section of the Machnozzle

through the fabric loses little of its thermal energy and can be passed through a condenser where it is mixed with cold water to yield a hot water source for the plant. Thus much of the energy in the steam can be recovered, making the predrying process more energy efficient.

While the Machnozzle may be operated with either steam or compressed air, the study was conducted using steam for two reasons. First, many textile mills may require additional compressor capacity in order to supply air at a sufficient pressure and flow rate to operate the Machnozzle. The total mill steam consumption would be reduced when steam is used to operate the Machnozzle. Second, much of the energy in the steam can be recovered using a condenser, but the energy in the air can not be reclaimed.

C. TEST APPARATUS AND PROCEDURE

A test system for evaluating the Machnozzle's performance was designed and constructed during Phase II (2) of the DOE project. However, several operational problems were encountered when the system was tested. Due to these problems, much of the early effort of Phase III was spent in developing the test apparatus into a workable piece of equipment. Photographs of the Machnozzle and the test apparatus are shown in Figures 2, 3, and 4.

As shown in Figure 5, the 400 mm (approximately 16 inch) Machnozzle is mounted in a framework along with a series of guide rolls. The nozzle jet is directed downward into a plenum which houses the steam condenser. A blower is used to pull the mixture of steam, air, and water through the condenser and to exahust the wet air outdoors. Initially, the plan was to use a continuous loop of fabric which would be dried by the Machnozzle then rewetted and dried again. This proved to be impractical given the limitations of this equipment.

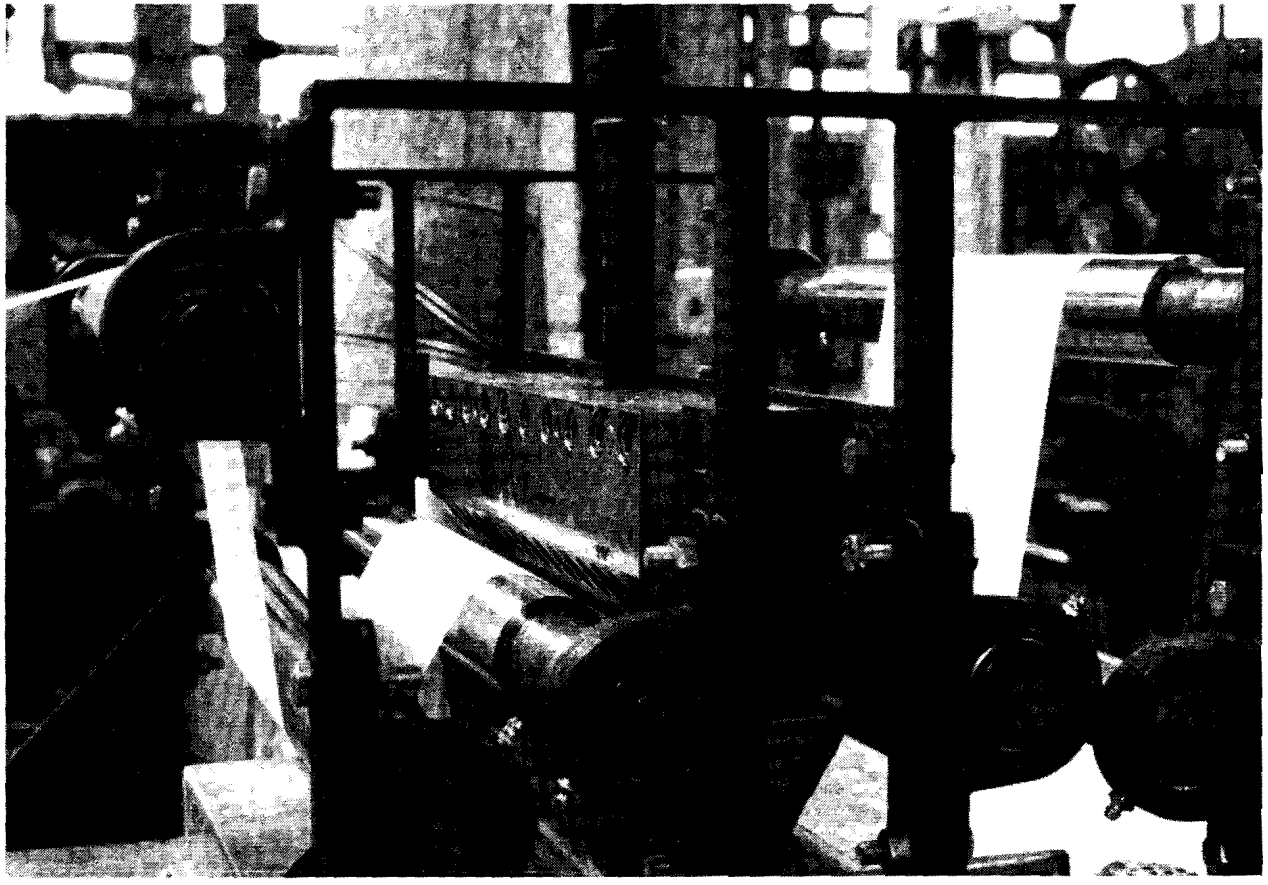

Figure 2. Machnozzle and Guide Rollers

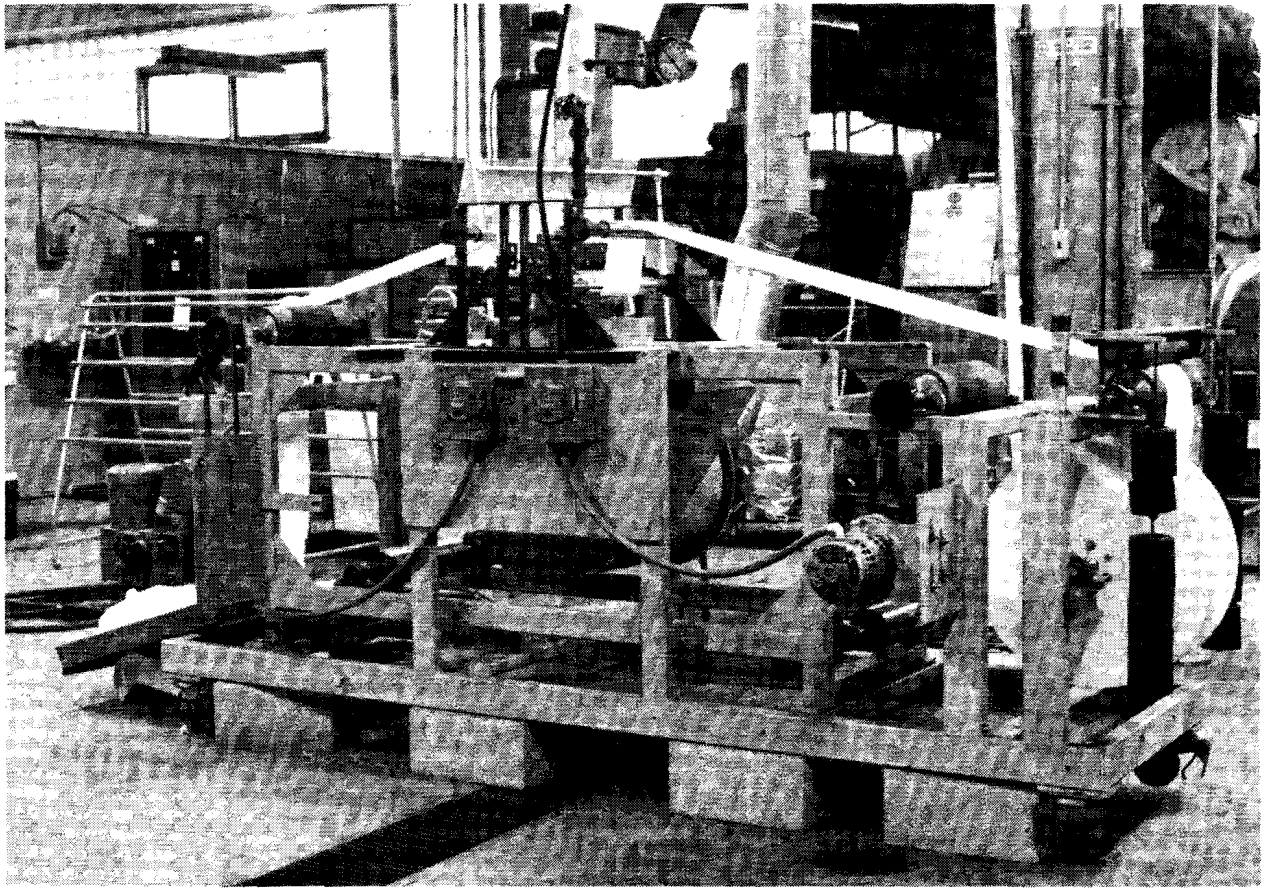

Figure 3. Fabric Being Tested on Machnozzle Apparatus

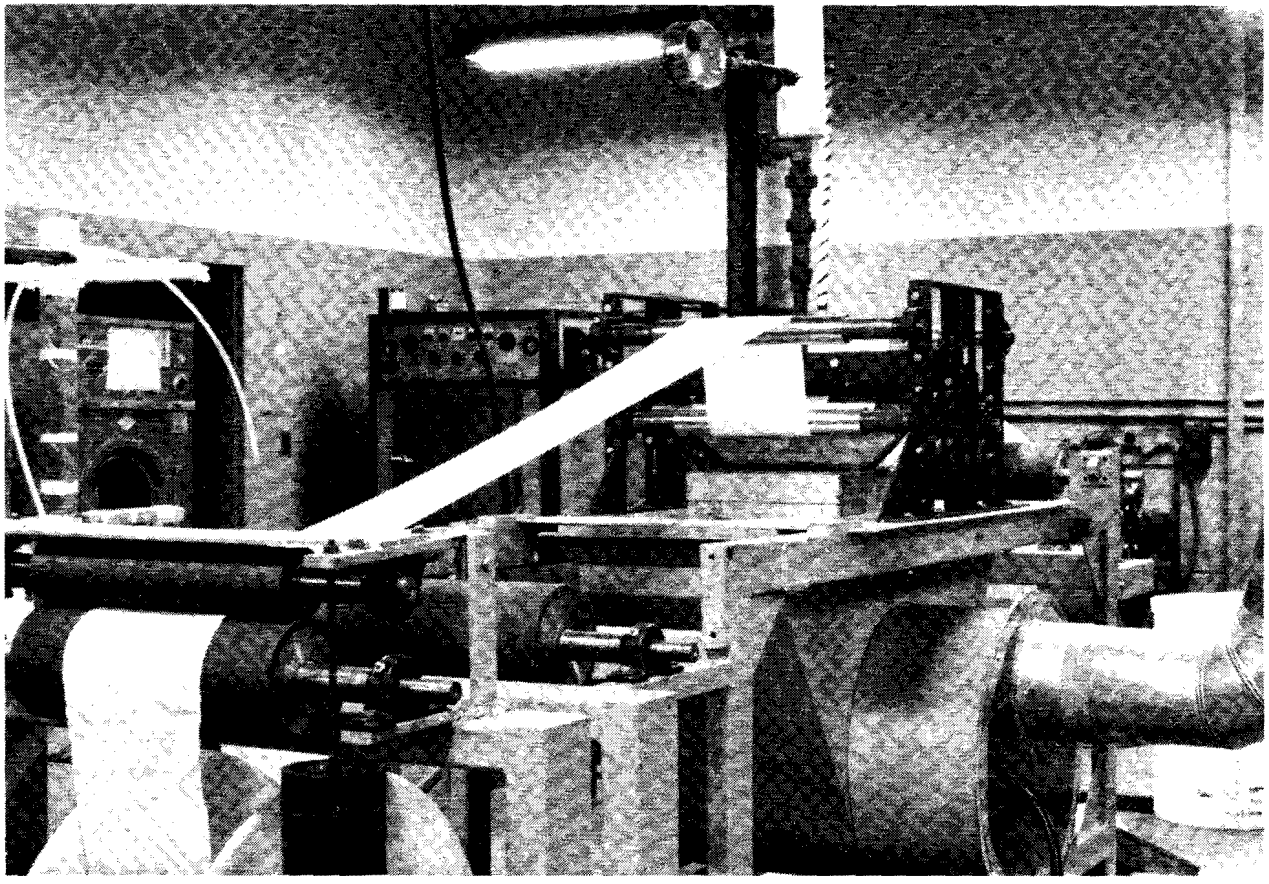

Figure 4. Rear View of Machnozzle Apparatus

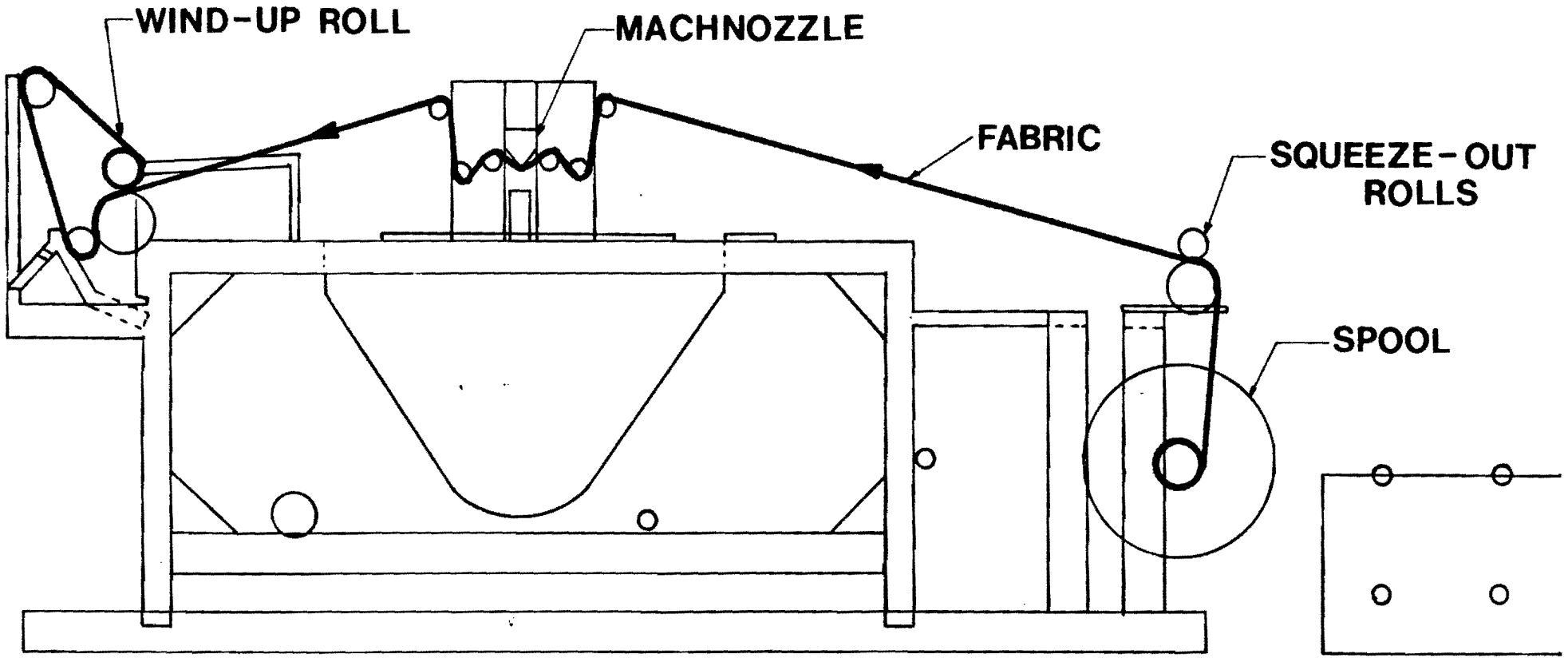

Figure 5. Test Set-Up

A spool was added at the wet end to hold the wet fabric. A take-up reel was later added at the dry end to ease the job of rewinding the fabric after a set of runs. Weighted squeeze rolls were used immediately before the Machnozzle to reduce the incoming moisture level of the fabric as would normally be the case in a mill. A set of drive rollers was used at the dry end of the machine to pull the fabric through the squeeze rolls and across the Machnozzle.

An electric resistance heated steam boiler was used to provide steam for the Machnozzle. Initial tests were hindered by the relatively imprecise control given by the simple on-off mechanical controllers. The wide variation in steam supply pressures resulted in a wide variation in steam flow rates through the Machnozzle. The mechanical controller was replaced by an electronic, proportional controller which is able to hold the steam supply pressure within less than 1 psi of the set point. This greatly reduced the fluctuation of the steam flow rate.

The normal test procedure was as follows (See Figure 5):

- Wind the fabric through the wet out tank onto the spool at the end of the machine. This operation is shown in Figure 6.
- Thread the fabric through the machine.
- Set the boiler controller at the given steam supply pressure and wait for it to reach that pressure.
- Turn on the steam line to the Machnozzle and allow the Machnozzle to heat up.
- Set the drive roller gear-motor for the given fabric speed.
- Turn on the fabric drive and run fabric through the machine for the specified period.

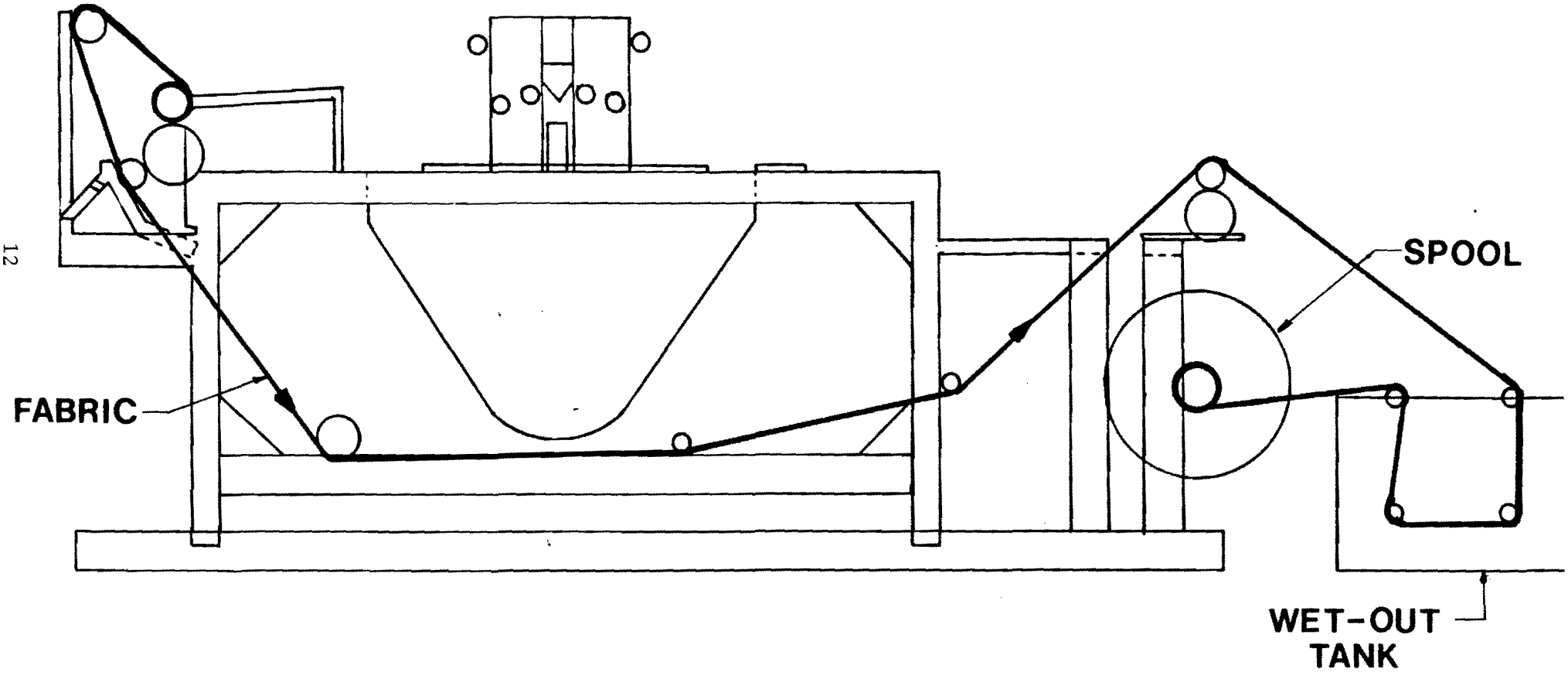

Figure 6. Wet-Out Set-Up

- Stop the machine and cut out fabric samples before and after the Machnozzle. Record relative humidity and steam flow rate. Sew the ends of the fabric together.
- Weigh the fabric samples then dry the fabric samples overnight in an oven and reweigh them.

A steam condensor system was installed in the plenum chamber below the Machnozzle on the test stand (See Figure 5). The first condenser consisted of two opposed rows of horizontal spray nozzles. Air and steam from the Machnozzle were pulled downward through the cold water spray by a fan which exhausts air from the plenum. Since this system did not work effectively, the two rows of spray nozzles were replaced by a series of baffles. Air and steam from the Machnozzle entered this chamber at the top, and a row of nozzles sprayed cold water into the steam at the top. Mixing of the steam and water continued as the water cascaded down the series of baffles. This condenser system yielded much greater performance than the two rows of spray nozzles.

D. TEST PLAN

The objective of the Machnozzle testing was to determine the performance and drying efficiency of the Machnozzle on common textile fabrics. The effects of the following parameters on the performance of the Machnozzle were studied:

- Fabric Type
- Fabric Speed
- Steam Supply Pressure

- Process Parameters
    1. wrap angle
    2. fabric tension
    3. incoming fabric temperature
    4. Machnozzle slot width

The tests to determine the effects of fabric type, fabric speed, and steam supply pressure are summarized in Table 1. These three types of fabrics, 100% cotton, 50/50 cotton/polyester, and 100% polyester were tested. Fabric speed was varied from 20 to 80 meters per minute, and steam supply pressures of 50, 75, and 95 psig were tested.

Early test runs during the development of the fabric transport system indicated that the fabric wrap angle (defined in Figure 7) was important in the performance of the Machnozzle. Therefore, a series of tests (see Table 2) were devised to investigate the effect of wrap angle on Machnozzle performance. After the effects of wrap angle on the Machnozzle's performance was established, tests (see Tables 3 and 4) were conducted in an attempt to determine why wrap angle is important. The interacting effects of wrap angle with both fabric tension and fabric temperature were tested.

The effect of Machnozzle slit width on Machnozzle performance was investigated. The tests conducted are summarized in Table 5.

Although the Machnozzle may be operated with either steam or compressed air, all of the tests were run using steam. The major reason for this was that much of the energy in the steam can be recovered, but the energy in compressed air cannot. Tests were conducted to determine how much of energy in the steam can be recovered by passing the steam through a condenser. The condenser

Table 1. Tests to Determine the Effects of Fabric Type, Fabric Speed, and Steam Supply Pressure

Fabric Type	Fabric Speed (m/min)	Steam Supply Pressure (psig)
50/50 PET/cotton 3.6 oz/yd^2	20	50, 75, 90
	60	50, 75, 90
	80	50, 75, 90
100% Cotton 4.0 oz/yd^2	20	50. 75, 90
	60	50, 75, 90
	80	50, 75, 90
100% PET 1.8 oz/yd^2	20	50, 75, 90
	60	50, 75, 90
	80	50, 75, 90

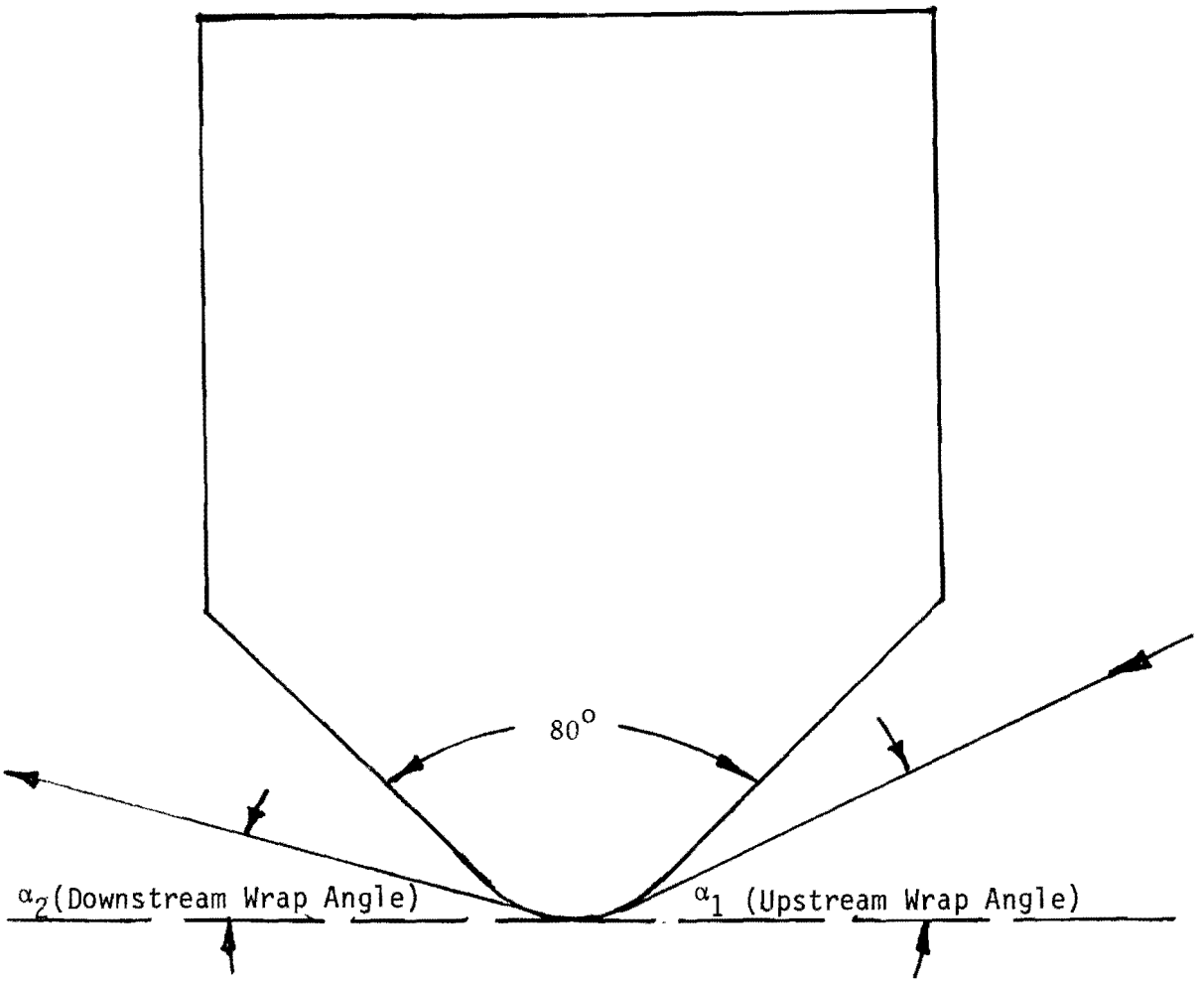

Figure 7. Fabric Wrap Angle

Table 2. Tests to Determine the Effect of Fabric Wrap Angle α.

Fabric Type	Fabric Speed (m/min)	Steam Supply Pressure (psig)	Upstream Wrap Angle α_1 (degrees)	Downstream Wrap Angle α_2 (degrees)
50/50 PET/cotton 3.5 oz/yd^2	80	95	17	17
			28	28
			47	47
			50	50
50/50 PET/cotton 3.5 oz/yd^2	80	95	17	50
			28	50
			47	50
50/50 PET/cotton 3.5 oz/yd^2	80	95	50	17
			50	28
			50	47

Table 3. Tests to Determine the Effect of Fabric Tension

Fabric Type	Fabric Speed (m/min)	Steam Supply Pressure (psig)	Upstream Angle α_1 (degrees)	Downstream Angle α_2 (degrees)	Tension Level
50/50 PET/cotton 3.5 oz/yd^2	80	95	50	50	Low Medium High
50/50 PET cotton	80	95	28	28	Low Medium High

Table 4. Tests to Determine the Effect of Fabric Temperature

Fabric Type	Fabric Speed (m/min)	Steam Supply Pressure (psig)	Upstream Wrap Angle α_1 (degrees)	Downstream Wrap Angle α_2 (degrees)
100% Cotton 5.7 oz/yd^2	80	95	28	130
			47	130
			50	130
			50	70

Table 5. Tests to Determine the Effect of Slit Width

Fabric Type	Fabric Speed (m/min)	Steam Supply Pressure (psig)	Wrap Angles $\alpha_1 = \alpha_2$ (degrees)	Slit Width (inches)
50/50 PET/COTTON 3.5 oz/yd^2	85	95	50	0.001 0.002

tests along with the results of the tests will be discussed in the results section of this report.

E. RESULTS

The results of the Machnozzle and condenser tests are summarized in this section. The full set of results for the Machnozzle tests is given in Appendix 1.

1. Effects of Fabric Type, Fabric Speed, and Steam Supply Pressure

The effectiveness of the Machnozzle in removing moisture from the three types of fabrics tested is shown in Figures 8, 9, and 10 for fabric speeds ranging from 20 to 80 m/min and a steam supply pressure of 95 psig. After passing through the squeeze rolls, 100% cotton fabrics weighing 4.0 oz/yd^2 had a moisture content (based on bone dry fabric weight) of approximately 97%. The Machnozzle reduced the moisture content to 34 and 46% for fabric speeds of 20 and 80 m/min, respectively. After passing through squeeze rolls, the moisture content of 50/50 cotton/polyester fabric weighing 3.6 oz/yd^2 was approximately 68%. The moisture content was reduced by the Machnozzle to 7 and 17% for fabric speeds of 20 and 80 m/min, respectively. The Machnozzle was extremely effective in removing moisture from 100% polyester fabric weighing 1.8 oz/yd^2. The moisture content was reduced from approximately 61% to 3 and 6% for fabric speeds of 20 and 80 m/min, respectively. The results showed that as the fiber in the fabric was changed from cotton to polyester, lower moisture contents were obtained using the Machnozzle. The results were expected since cotton is hydrophilic while polyester is hydrophobic.

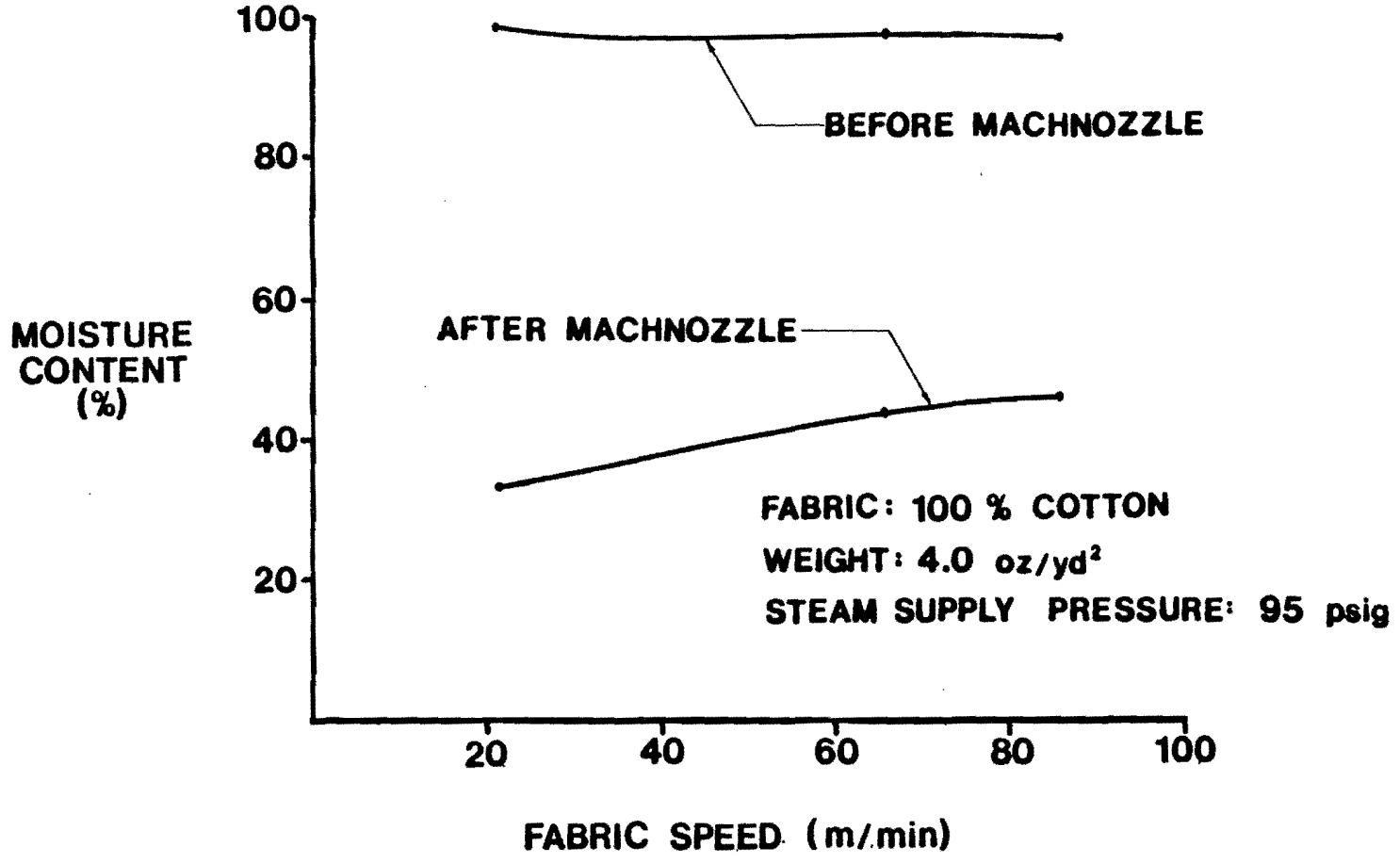

Figure 8. Fabric Moisture Content versus Fabric Speed Before and After the Machnozzle for 100% Cotton Fabric

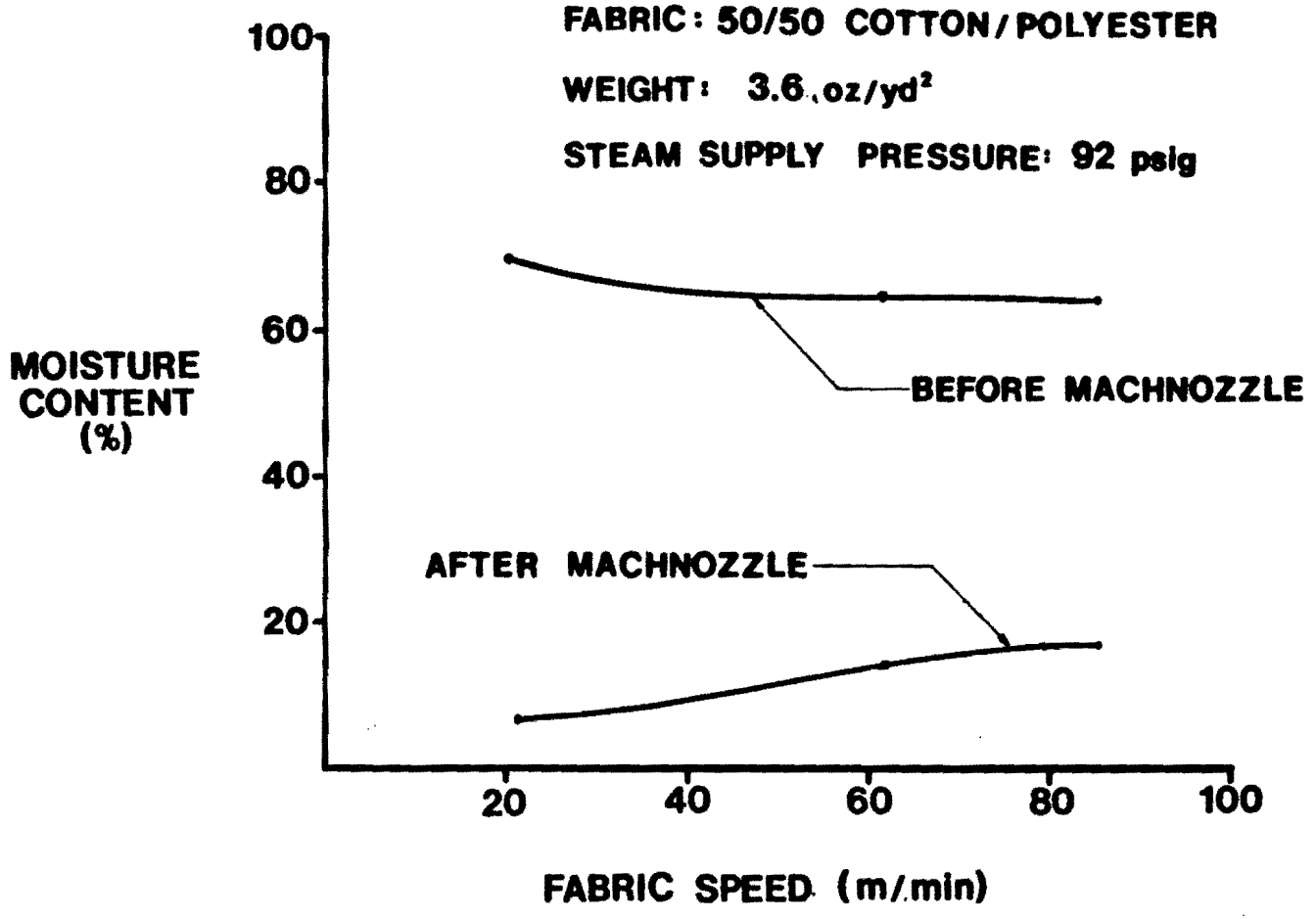

Figure 9. Fabric Moisture Content Versus Fabric Speed Before and After the Machnozzle for 50/50 Cotton/Polyester Fabric

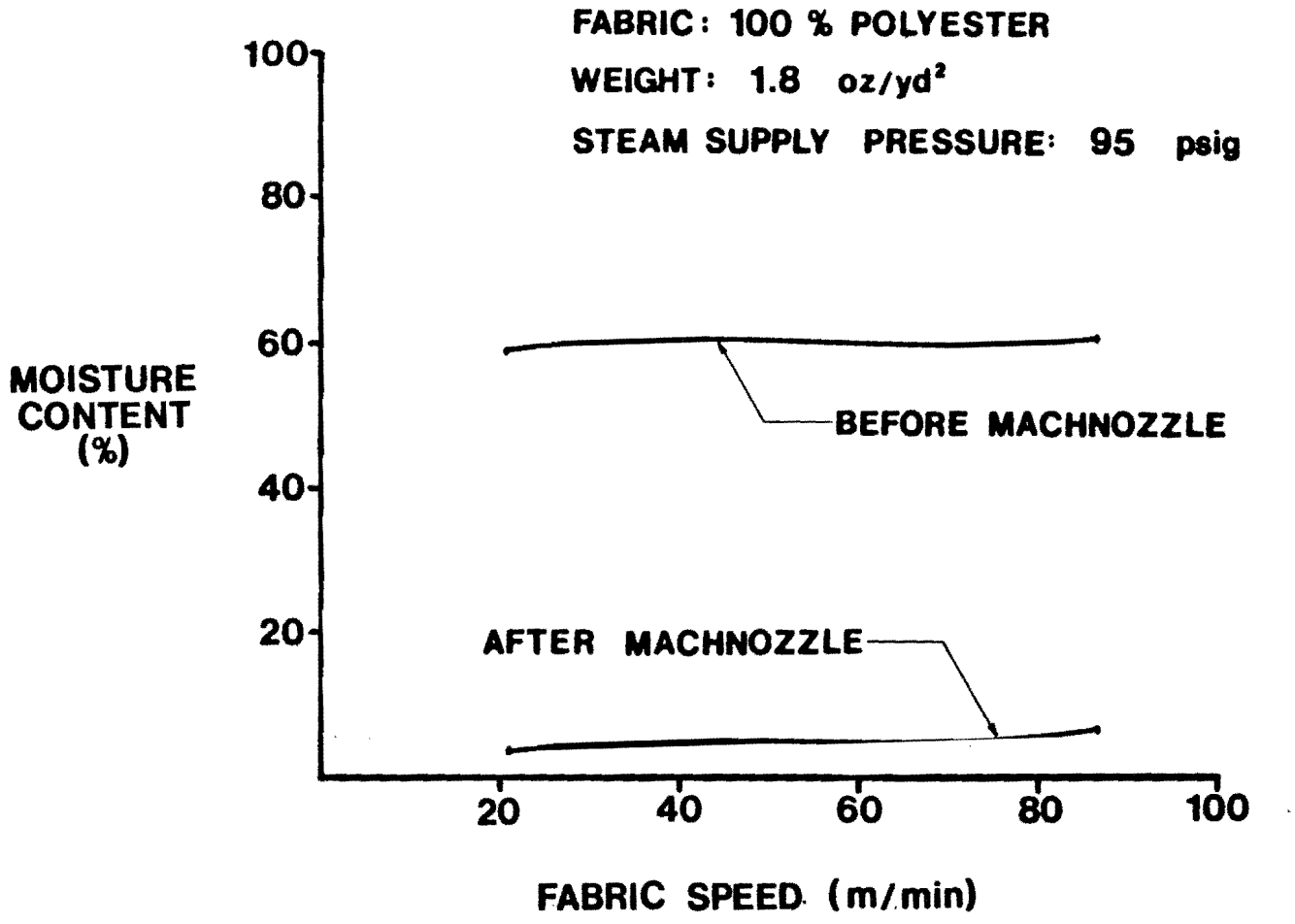

Figure 10. Fabric Moisture Content versus Fabric Speed Before and After the Machnozzle for 100% Polyester Fabric

The effect of increasing fabric speed can be seen in Figures 8 through 13. As fabric speed is increased, moisture removal is decreased slightly. Even though the moisture level exiting the Machnozzle is slightly lower at the lower fabric speeds, the Machnozzle is more energy efficient at the higher speeds. This results from productivity increasing linearly with fabric speed while steam consumption increases only slightly with fabric speed.

The effect of increasing the steam supply pressure on fabric moisture content after the Machnozzle is illustrated in Figures 11, 12, and 13. Plots of moisture contents in each of the three fabrics versus fabric speed are given for steam supply pressures of 50, 75, and 95 psig. As steam supply pressure is increased, moisture content is reduced. For example, for the cotton fabric at a fabric speed of 80 m/min moisture content was reduced from 62 to 46% as steam supply pressure was increased from 50 to 95 psig.

2. Effects of Other Process Parameters

During the early development of the Machnozzle test stand, the importance of the fabric wrap angle on Machnozzle performance became apparent. A series of tests were run to determine the effect of fabric wrap angle on Machnozzle performance. Figure 14 defines the upstream or entering wrap angle and the downstream wrap angle. The wrap angle experiments were run on 50/50 PET/cotton fabric weighing 3.5 oz/yd^2. All the runs were made at 80 m/min with a steam supply pressure of 95 psig.

The first series of tests were run with equal upstream and downstream wrap angles. Table 6 shows the results of these runs. As the wrap angles

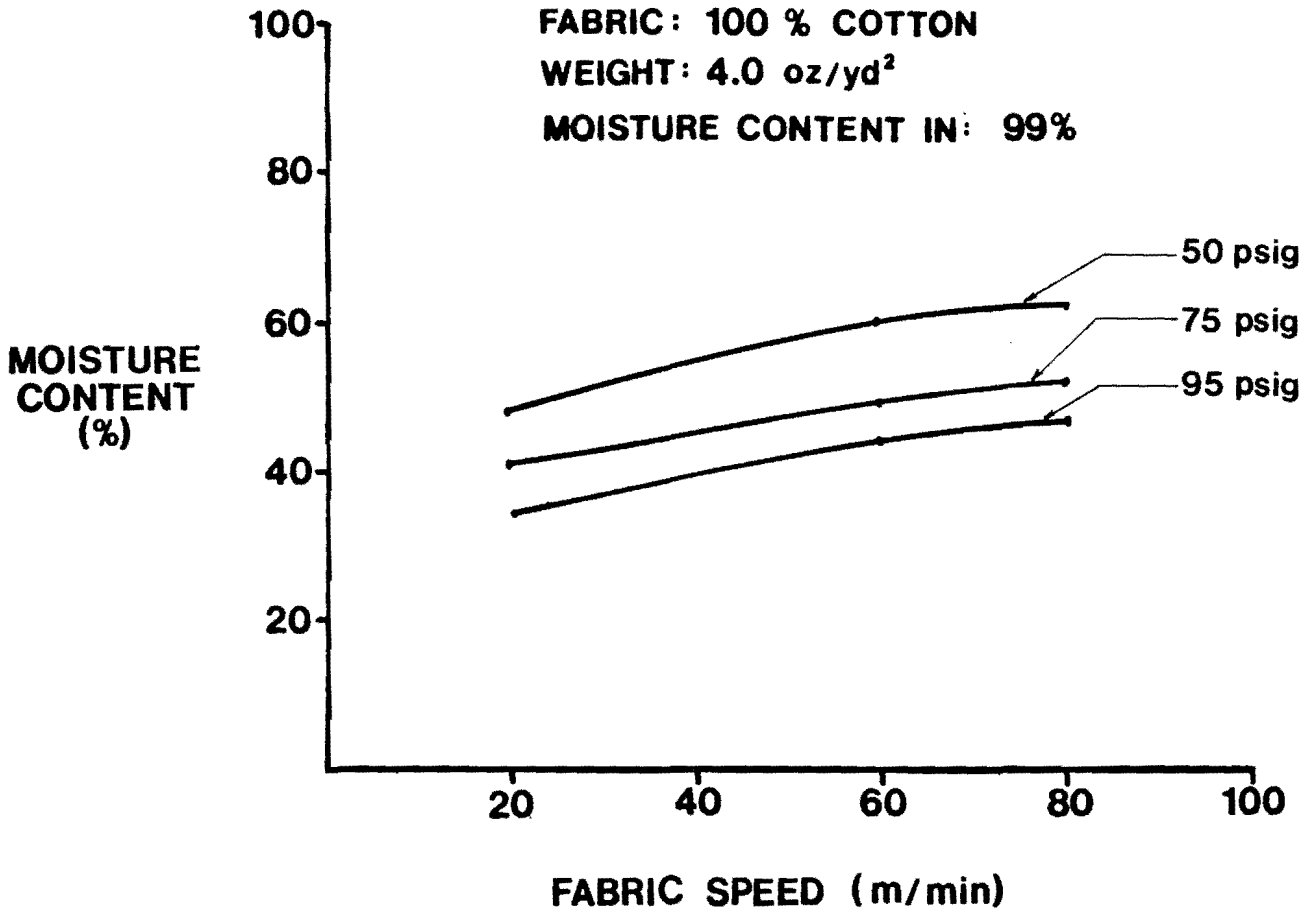

Figure 11. 100% Cotton Fabric Moisture Content Exiting the Machnozzle for Three Steam Supply Pressures

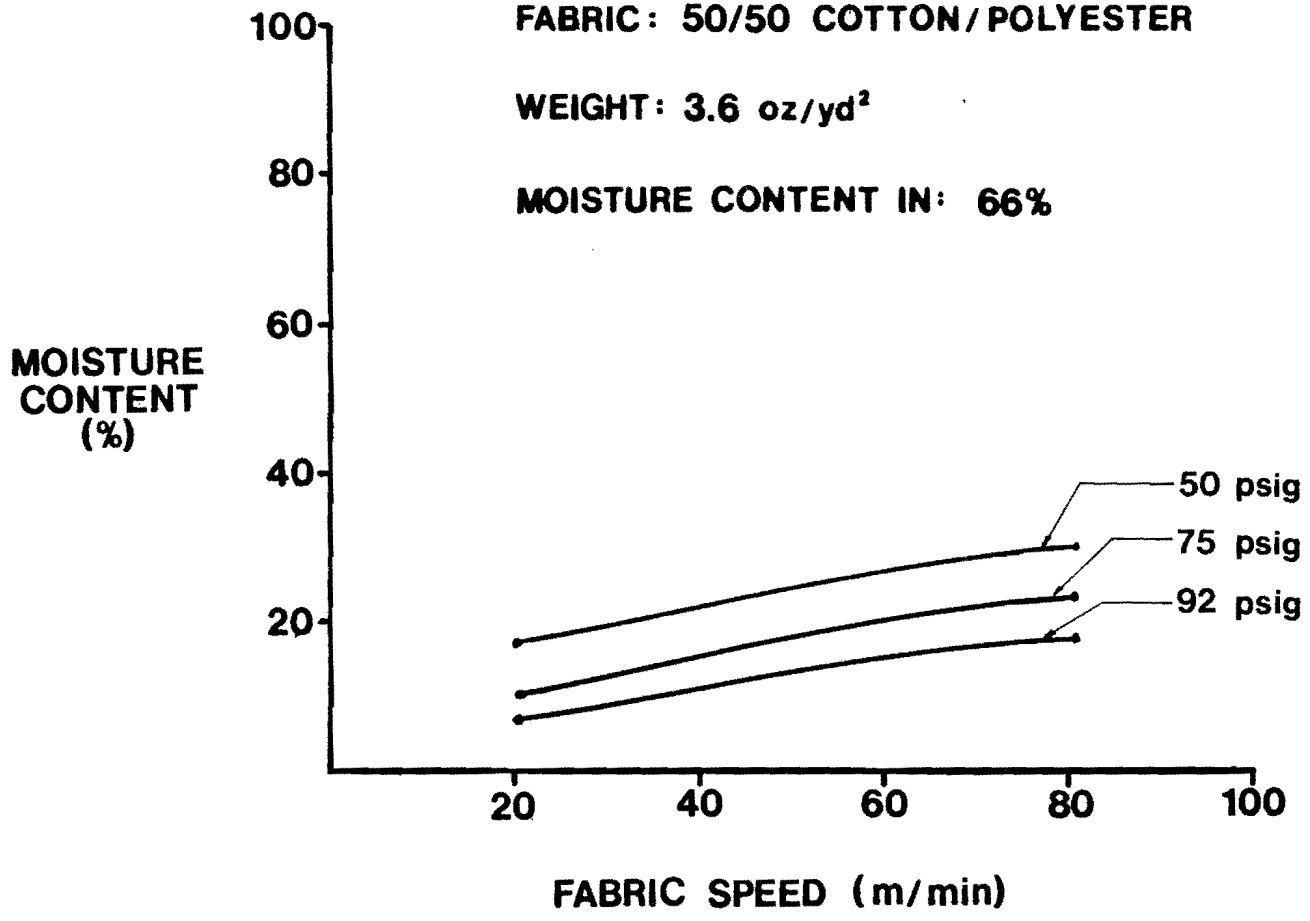

Figure 12. 50% Cotton/50% Polyester Fabric Moisture Content Exciting the Machnozzle for Three Steam Supply Pressures

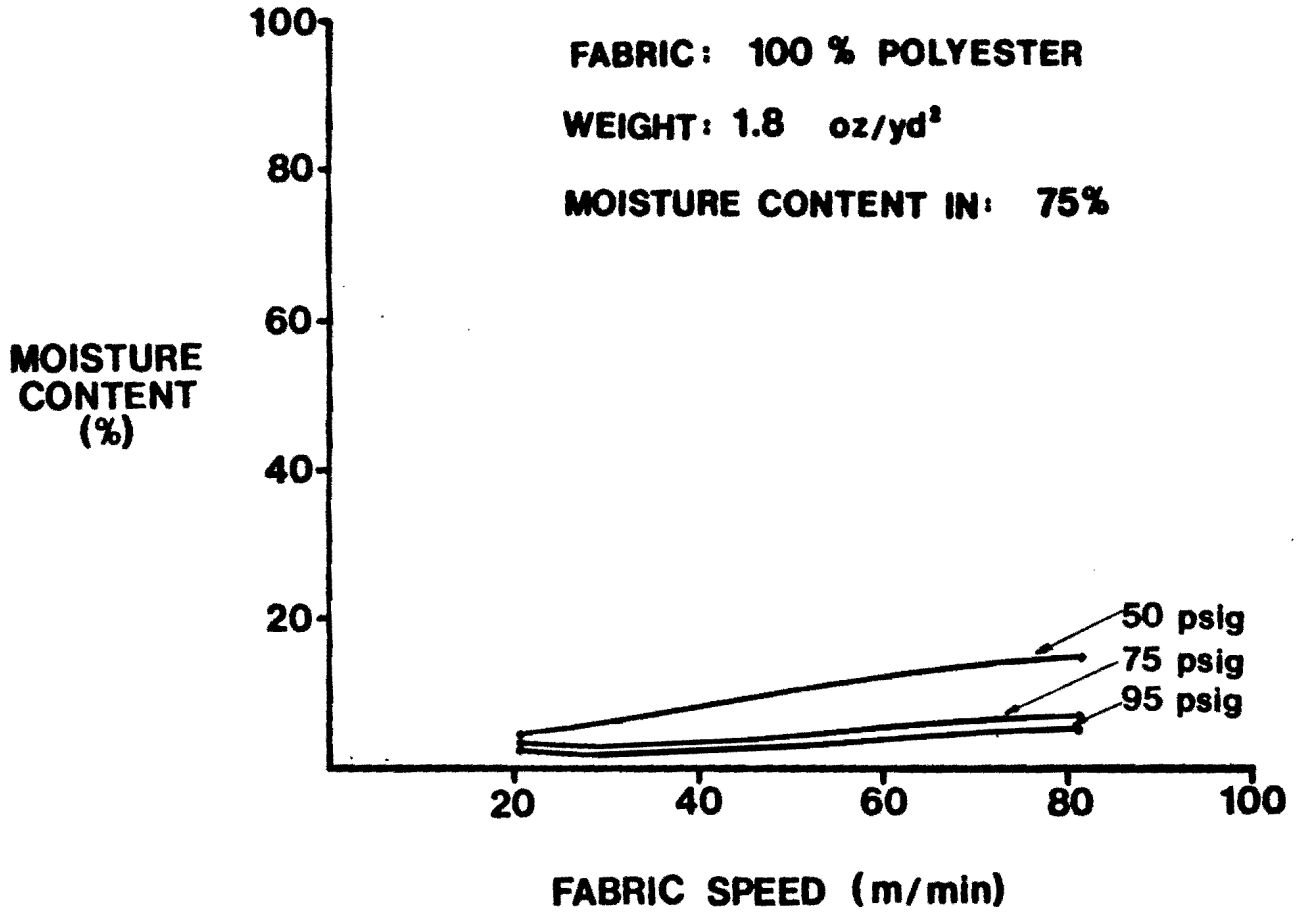

Figure 13. 100% Polyester Fabric Moisture Content Exiting the Machnozzle for Three Steam Supply Pressures

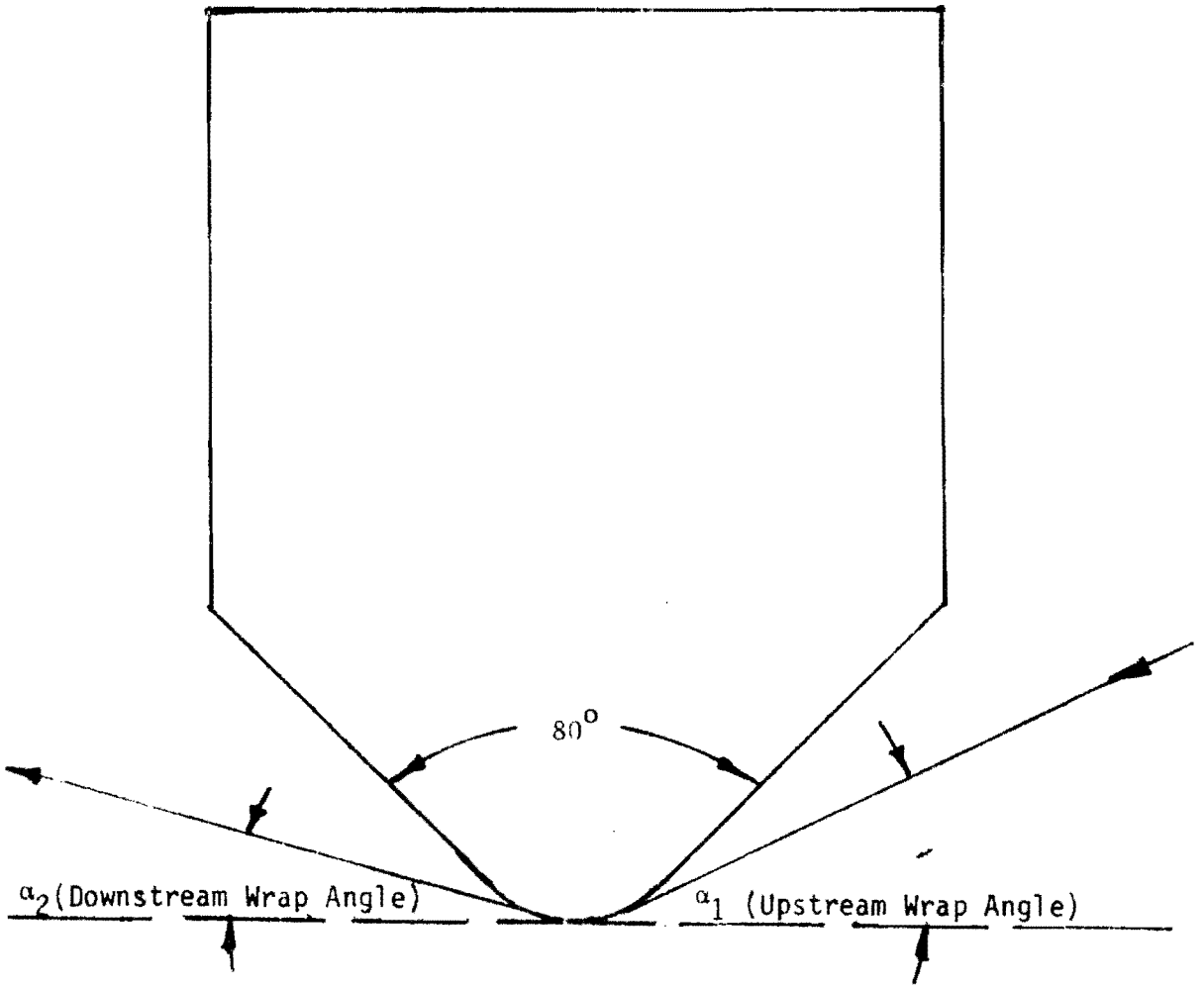

Figure 14. Fabric Wrap Angle

Table 6. Effect of Wrap Angle on Moisture Content

α_1	α_2	MOISTURE CONTENT OUT (%)
17	17	56
28	28	56
47	47	49
50	50	29

FABRIC: 50/50 COTTON/POLYESTER

WEIGHT: 3.5 oz/yd^2

SPEED: 80 m/min

MOISTURE CONTENT IN: 66 %

STEAM PRESSURE: 95 psig

were increased from 17^{o} to 47^{o}, there was slight improvement in the drying performance of the Machnozzle. As the wrap angles were increased from 47^{o} to 50^{o} where the fabric touches both faces of the Machnozzle, the drying performance improved greatly.

Two series of tests were run to investigate the importance of the fabric touching the upstream and downstream faces of the Machnozzle. Table 7 shows the results of the tests with the fabric touching the downstream face. The drying performance is much better when the fabric touches the upstream face than when the upstream wrap angle is 28^{o} or 47^{o}. Table 8 shows the results of the tests with the fabric touching the upstream face of the Machnozzle. The downstream wrap angle has little effect on the drying performance of the Machnozzle when the fabric touches the upstream face.

One possible explanation for the importance of the fabric touching the upstream face of the Machnozzle is that the drag on the fabric moving across the face of the Machnozzle increases the tension of the fabric at the Machnozzle slot which opens up the fabric, making dewatering easier. To test this hypothesis, a test was run to determine the effect of fabric tension on the drying performance of the Machnozzle. This test was run on 100% cotton fabric weighing 4.0 oz/yd^{2} at 80 m/min with a steam supply pressure of 95 psig. Runs were made with the upstream wrap angle at 28^{o} and 50^{o} (i.e., with the fabric touching the upstream face) for three fabric tension levels: low, medium, and high. The wrap angles for this test are illustrated in Figures 15, and the results are presented in Figure 16. The results showed that while fabric tension has a slight effect on Machnozzle drying performance, fabric wrap angle has a much larger effect.

Table 7. Effect of Upstream Wrap Angle on Moisture Content

α_1	α_2	MOISTURE CONTENT OUT (%)
28	50	40
47	50	37
50	50	29

FABRIC: 50/50 COTTON/POLYESTER

WEIGHT: 3.5 oz/yd^2

SPEED: 80 m/min

MOISTURE CONTENT IN: 66 %

STEAM PRESSURE: 95 psig

Table 8. Effect of Downstream Wrap Angle on Moisture Content

α_1	α_2	MOISTURE CONTENT OUT (%)
50	28	26
50	47	24
50	50	29

FABRIC: 50/50 COTTON/POLYESTER

WEIGHT: 3.5 oz/yd^2

SPEED: 80 m/min

MOISTURE CONTENT IN: 66 %

STEAM PRESSURE: 95 psig

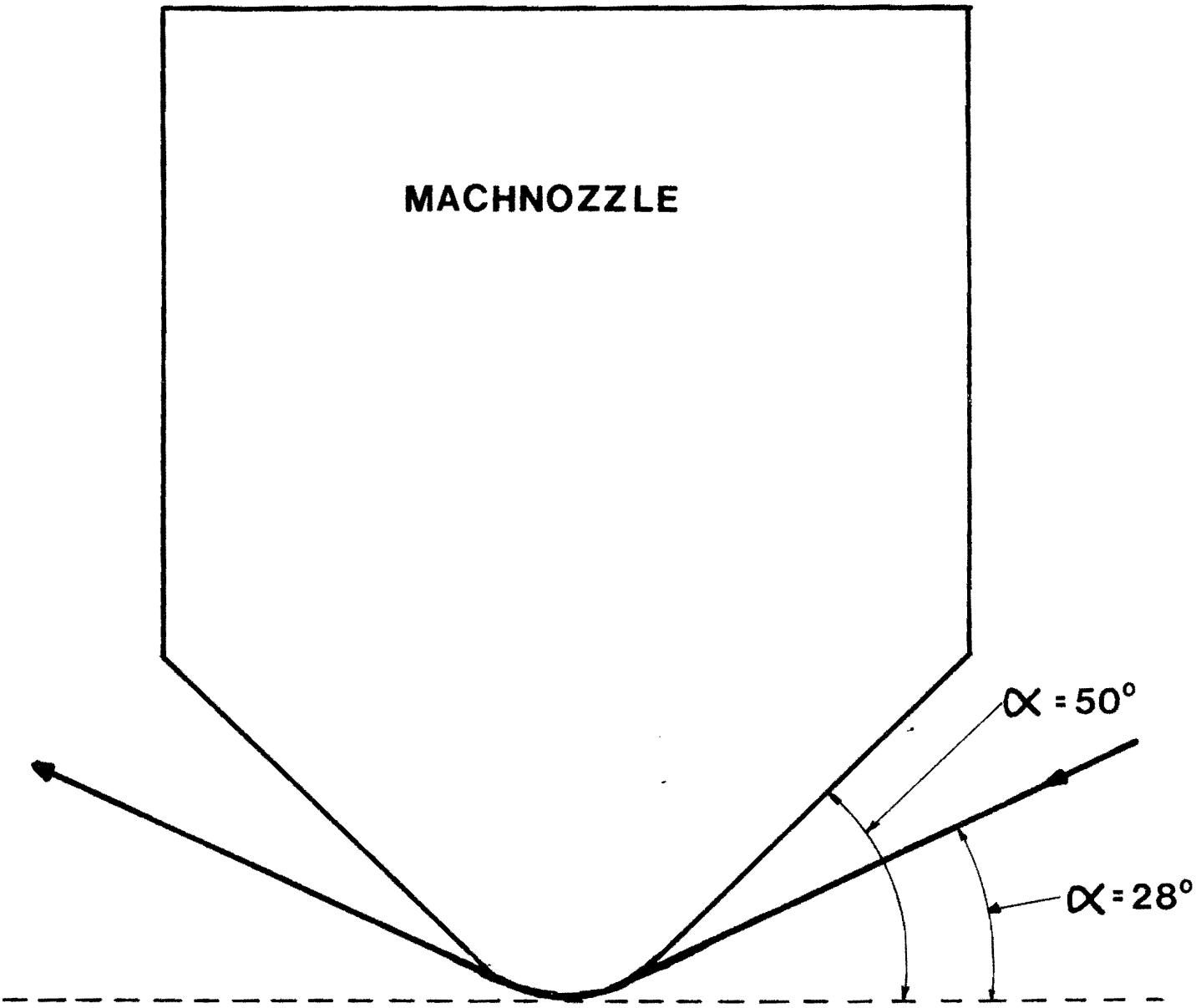

Figure 15. Wrap Angles for Fabric Tension Test

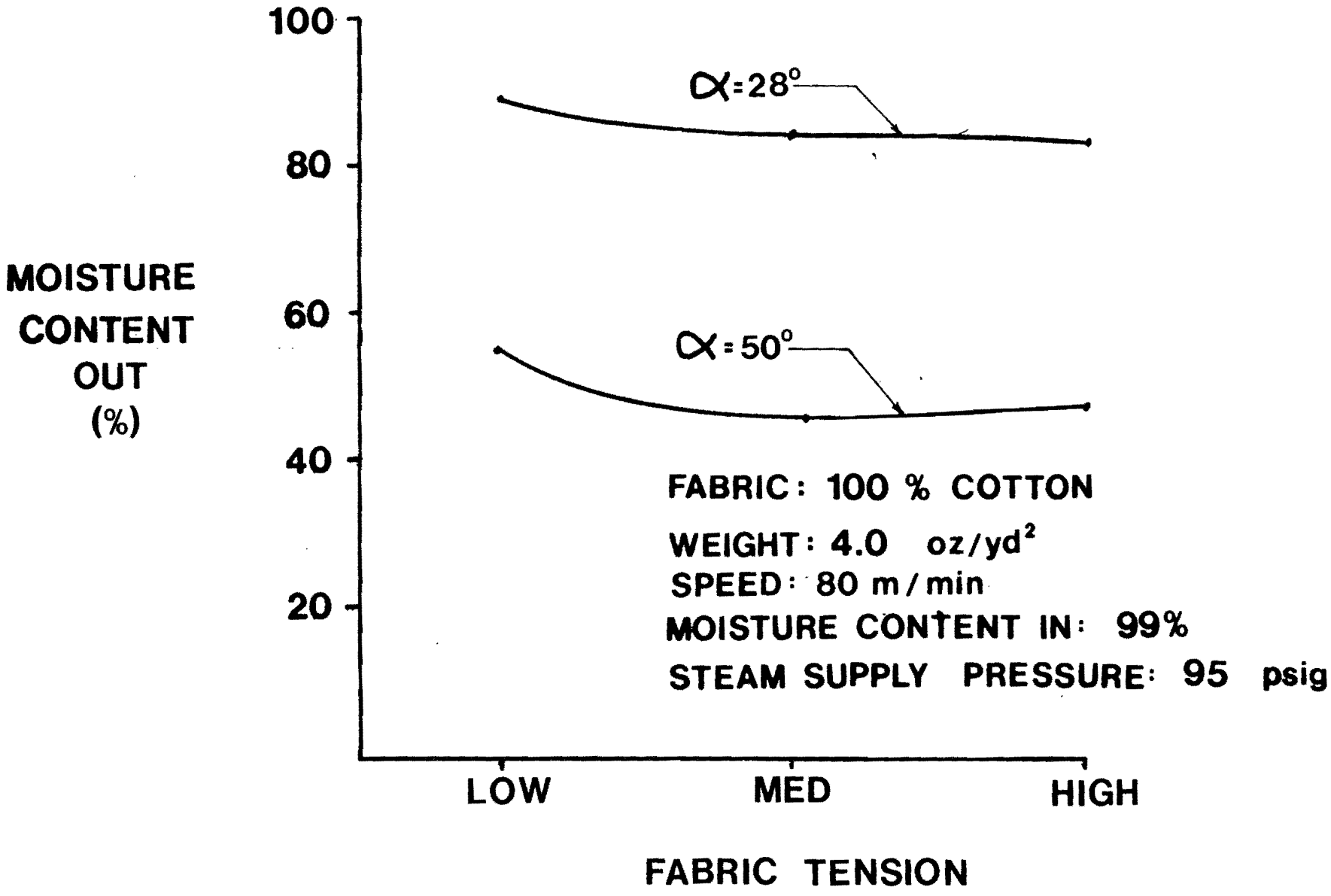

Figure 16. Effect of Fabric Tension on Moisture Content

Another possible explanation for the importance of the fabric touching the upstream face of the Machnozzle is that the hot face of the Machnozzle heats the water in the fabric, thereby reducing the surface tension and viscosity of the water, thus making the water easier to remove. To test this hypothesis, a test was run to determine the effect of incoming fabric temperature on Machnozzle performance. The fabric was wet out in boiling water; however, by the time the fabric reached the Machnozzle, the fabric had cooled to 130°F. The results of this test (see Table 9) indicate that while incoming fabric temperature does have a slight effect on Machnozzle drying performance, fabric wrap angle has a much larger effect.

Thus, test results showed that both hypotheses explaining the importance of fabric wrap angle were inadequate. While the reason for the importance of fabric wrap angle is still unclear, the importance of fabric wrap angle has been clearly demonstrated.

A test was run to determine the effect of the Machnozzle slit width on the drying performance of the Machnozzle. A 0.001-inch stainless steel shim was used to increase the Machnozzle slit width from approximately 0.001 to 0.002 inches. The test was run on 50/50 PET/cotton fabric weighing 3.5 oz/yd^2, at 80 m/min and with a steam supply pressure of 95 psig. The results of this test are shown in Table 10. Increasing the slit width had little effect on drying; however, the steam flow rate of the Machnozzle was approximately doubled. Therefore, the energy consumption per weight of fabric processed doubled when the slit width was doubled. The results suggest that Machnozzle drying energy

Table 9. Effect of Fabric Temperature on Moisture Content

α_1	MOISTURE CONTENT OUT %	FABRIC TEMP. IN °F
28	85	130
47	85	130
50	63	130
50	70	70

FABRIC: 100 % COTTON

WEIGHT: 5.04 oz/yd^2

SPEED: 80 m/min

MOISTURE CONTENT IN: 93 %

STEAM PRESSURE: 95 psig

Table 10. Effects of Slit Width on Moisture Content

SLIT WIDTH (inches)	MOISTURE CONTENT OUT (%)
0.001	26
0.002	27

FABRIC: 50/50 COTTON POLYESTER
WEIGHT: 3.5 oz/yd
SPEED: 80 m/min
MOISTURE CONTENT IN: 66%
STEAM PRESSURE: 95 psig

efficiency could be increased by decreasing the slit width further. However, reducing the slit width below 0.001 inch was beyond the scope of the project since modifications of the Machnozzle would have been necessary.

3. Condenser Tests

The results of one series of condenser tests are summarized in Table 11. Both the amount of energy recovered in the condenser and the temperature of the heated water leaving the condenser depend on the flow rate of cold water fed to the condenser. At condenser operating conditions giving the highest heat recovery (69%), the temperature of the heated water was 118°F. The maximum heated water temperature (130°F) occurred at a lower cold water flow rate. The heat recovery corresponding to the heated water temperature of 130°F was 27%.

Hot water can be used to charge heat conducting cylinders or dryer cans. Water, at temperature between 140 and 180°F, provides significant drying effects (2). One of the objectives of the research reported herein was to determine if the heated water from the Machnozzle condenser system could be used to charge drying cylinders. The maximum temperature of the heated water from the condenser was 130°F which is not sufficient for economical drying. Accordingly, this approach was abandoned. However, there are usually one or more washing steps prior to drying that require warm water at approximately 100°F. The energy recovered from the Machnozzle predrying step can be utilized in many cases in the washing steps.

Table 11. Results of Condenser Test

Cold Water Flow Rate (gal/hr)	Exhaust Water Temperature (^{o}F)	Energy Recovered	
		(BTU/hr)	(%)
29	128	13,180	13
59	130	27,560	27
103	116	36,030	36
189	118	69,530	69
212	102	49,450	40

Note: Machnozzle steam flow rate was 90 lb/hr.
Machnozzle Rate of Energy Consumption was 100,000 BTU/hr.
Cold Water Temperature was 74^{o}F.

F. STEAM CONSUMPTION

The steam consumed in removing a pound of water varies with fabric speed and steam supply pressure as shown in Figures 17 and 18. The steam consumption per pound of water removed decreased as fabric speed was increased even though lower moisture contents were obtained at lower fabric speeds. The reason is that the rate at which steam is consumed by the Machnozzle is nearly constant and independent of fabric speed. As fabric speed is increased, the quantity of fabric processed per unit time by the Machnozzle increases. As a result, steam consumption per pound of water removed decreases as fabric speed is increased. As steam supply pressure is increased, steam consumption increases at low fabric speeds. However, at a fabric speed of 80 m/min, there is little difference in steam consumption per pound of water removed from the cotton fabric. Since more moisture is removed at the steam pressure of 95 psig, the Machnozzle would probably be operated at 95 psig or higher under commercial conditions for 100% cotton fabric. The Machnozzle steam consumption per pound of water removed was significantly higher at 95 psig than at 50 psig for the 100% polyester fabric. The Machnozzle was actually over drying the fabric at 95 psig and would operate at a lower pressure on polyester fabric in a mill.

The steam consumption for a fabric speed of 80 m/min was approximately one pound of steam per pound of water removed. The steam requirements of steam can dryers are normally between 1.5 and 2.0 pounds of steam per pound of water removed. Thus the low steam requirements of the Machnozzle suggest that this device has a potential for saving energy in the fabric drying process.

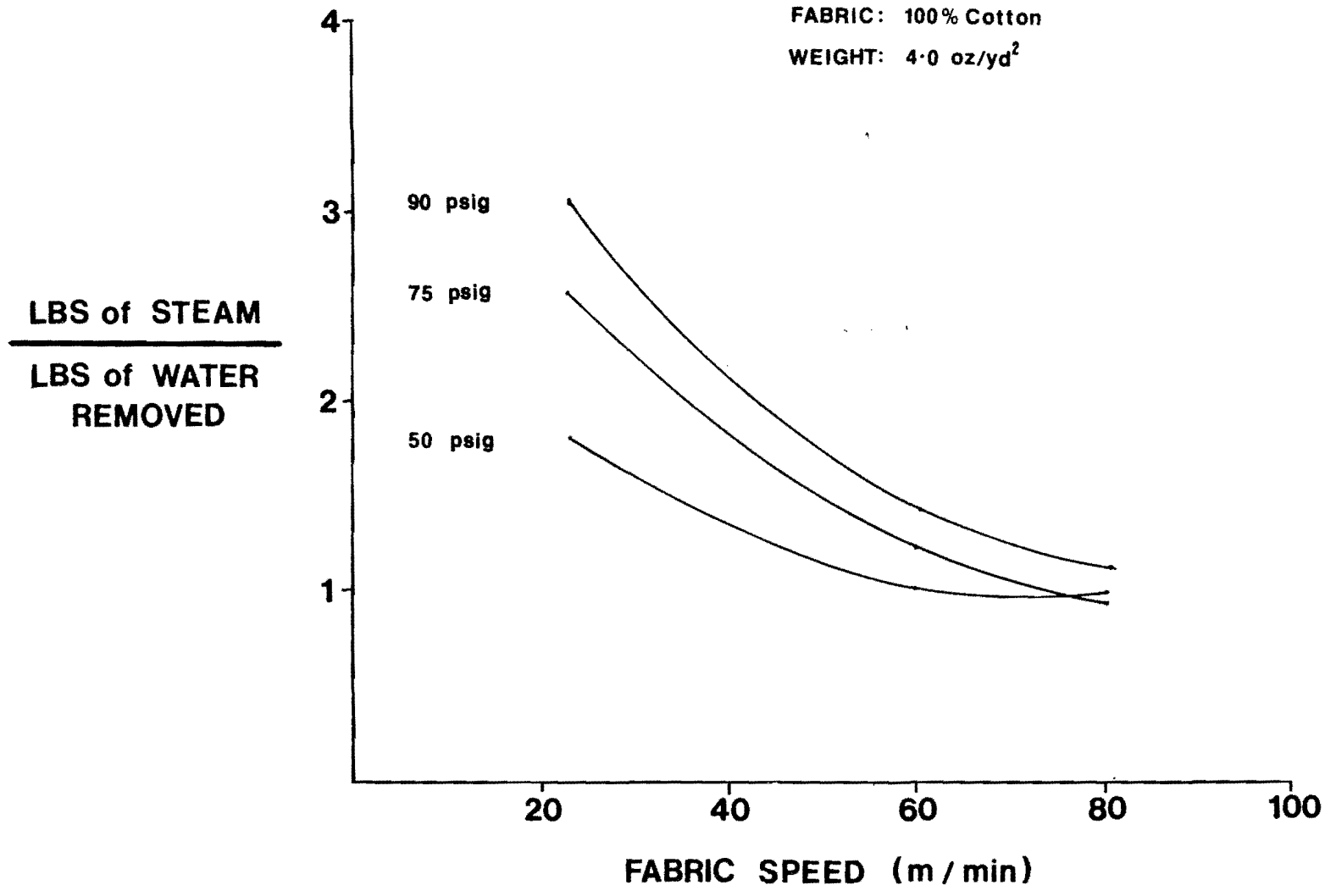

Figure 17. Steam Requirements for 100% Cotton Fabric

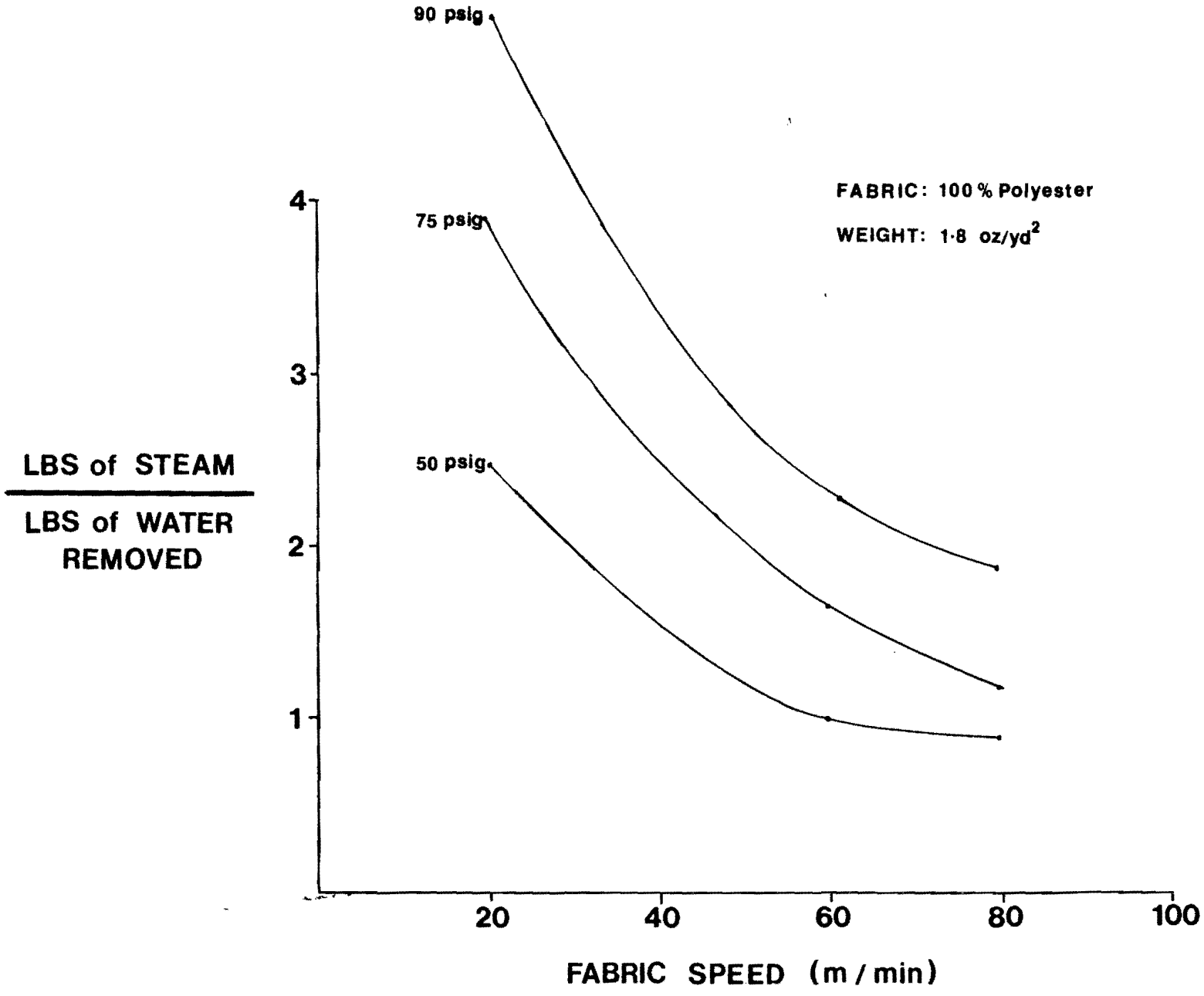

Figure 18. Steam Requirements for 100% Polyester Fabric

When the energy recovered by the condenser is considered, the Machnozzle becomes even more attractive as a device for predrying fabrics. The results of condenser tests (see Table 11) indicate that approximately 69% of the energy in the steam used by the Machnozzle can be recovered. If a condenser with a recovery efficiency of 69% is used, the steam consumption of the Machnozzle is shown in Figure 19. At a fabric speed of 80 m/min, the steam consumption of the Machnozzle is approximately 0.3 pounds of steam per pound of water removed.

G. ECONOMIC ANALYSIS

The test results show clearly that the Machnozzle can significantly reduce the moisture content in fabrics. However, if the Machnozzle is to be utilized by the textile industry, the Machnozzle must also be economically attractive. Therefore, an economic analysis of the Machnozzle as a fabric predrying device has been made. The parameter used to judge the economic performance of the Machnozzle was Internal Rate of Return (IRR).

The first step of the analysis was to determine the reduction in energy consumption obtained by utilizing the Machnozzle as a predrying device instead of conventional methods. The two common devices used to predry fabrics are steam cans and infrar-red dryers. Typical energy requirements for steam can and infra-red dryers are 1.5 to 20 and 3.0 to 4.0 pounds of steam per pound of water removed, respectively. For the purposes of the analysis, the Machnozzle has been compared with a steam can system that consumes 1.5 pounds of steam per pound of water removed.

The decrease in the rate of steam consumption ($\Delta\dot{M}$) obtained with the Machnozzle, assuming no heat recovery, is

$$\Delta\dot{M} = \rho_f V_f W_f \ (\gamma_{in} - \gamma_{out}) \ (E_S - E_M) \qquad (1)$$

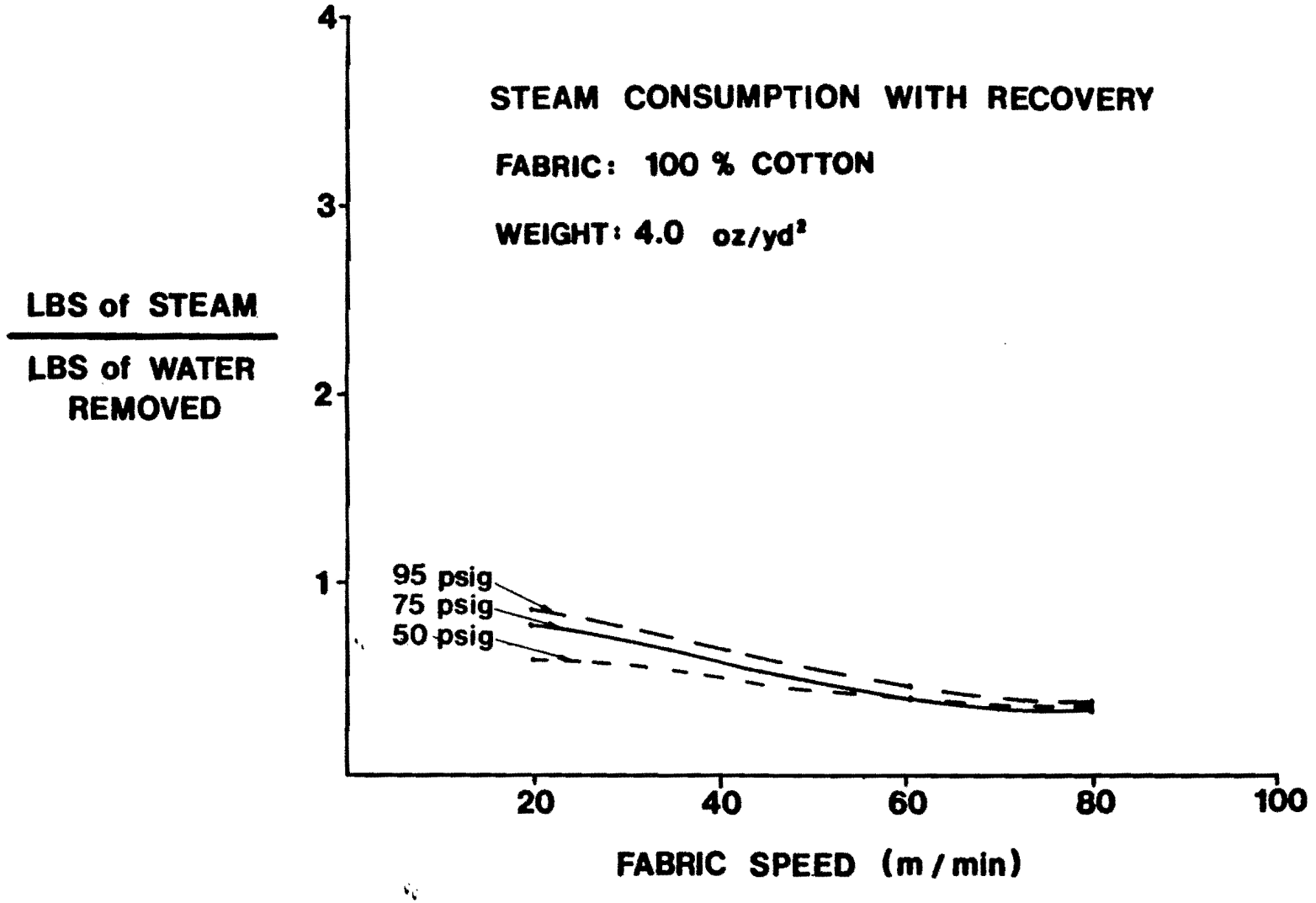

Figure 19. Steam Requirements with Heat Recovery for 100% Cotton Fabric

where

ρ_f = weight of fabric per surface area (lb/yd^2)

V_f = linear speed of fabric (yd/hr.)

W_f = width of fabric (yd)

γ_{in} = moisture content before Machnozzle (lbs of water/lb of fabric)

γ_{out} = moisture content after Machnozzle (lbs of water/lb of fabric)

E_M = steam requirement of Machnozzle (lbs of steam/lbs of water removed)

E_S = steam requirement of steam cans (lbs of steam/lbs of water removed)

When heat recovery is included, the decrease in the rate of steam consumption is given by the relationship

$$\left(\Delta\dot{M}\right)_R = \rho_f V_f W_f \left(\gamma_{in} - \gamma_{out}\right)\left(E_S - E_M(1-R)\right) \tag{2}$$

where

R = fraction of heat recovered

The expressions for the annual cash in flow $(CF)_{in}$ generated by using the Machnozzle with and without heat recovery are

$$(CF)_{in} = s\,(\Delta\dot{M})\,t \tag{3}$$

and

$$\left((CF)_{in}\right)_R = S(\Delta\dot{M})_R\ t \tag{4}$$

where

S = cost of steam ($/lb of steam)

t = number of operating hours per year

The annual cash outflow required for maintaining the Machnozzle is simply

$$(CF)_{out} = F$$

where

F = annual maintenance cost

The Internal Rate of Return (IRR) is defined as the discount rate which reduces to equality present values of expected cash outflows to present values of expected cash inflows (5) or

$$\left[\text{Present Values of Outflows}\right] = \left[\text{Present Values of Inflows}\right] \tag{5}$$

The present values of the outflows is the sum of the initial cost of the Machnozzle (and recovery system if used) plus the present value of all the maintenance cost. Thus

$$\left[\text{Present Value of Outflows}\right] = P + F\ (\text{pwf-}i\%\text{-}n) \tag{6}$$

where

P = initial cost of the Machnozzle (and recovery system if used)

pwf-i%-n = uniform series present worth factor which converts a uniform series of payments (or receipts) continuing for M periods to the entire series' equivalent present worth at a discount rate $\underline{i}$

If the cost of energy is constant, the annual cash inflow generated by using the Machnozzle is a simple uniform series. Thus, the present value of the cash inflows is given by the simple relationship

$$\left[\text{Present Value of Inflows}\right] = (CF)_{in}\ (\text{pwf-}i\%\text{-}n) \tag{7}$$

Substituting Equations (3) (or (4) if applicable), (6) and (7) into (5) and rearranging gives

$$\text{pwf-}i\%\text{-}n = \left(S(\Delta\dot{M})t - F\right)\Big/P \tag{8}$$

Equation (8) can be used to determine pwf-i%-η. Since η(the life of the Machnozzle in years) will be specified, standard interest tables and the value of pwf-i%-η can be used to determine $\underline{i}$ which is equivalent to the Internal Rate of Return (IRR).

The cost of energy for part of the analysis is not uniform, but increases at a rate of 10% per year. For those cases, the cost of energy is given by the equation

$$S = S_o + 0.1S_o(y-1) \tag{9}$$

where S_o = the cost of energy during the first year

y = an integer corresponding to the year in which the cost of energy is calculated

By substituting the relationship for S into Equation (3) (or 4) where applicable), the following equation for the annual cash inflow can be obtained

$$(CF)_{in} = S_o(\Delta\dot{M})t + 0.1S_o(\Delta\dot{M})(t)(y-1) \tag{10}$$

The first term in Equation (10) is a constant, and the second term increases linearly with (y-1). Thus, the annual cash inflow can be separated into two terms. The first term corresponds to a uniform series of cash inflows, and the second to a gradient series that increases by the same amount each year. The total present value of the annual cash inflows can be written as the sum of the present values of the two terms, that is

$$\left[\text{Present Value of Inflows}\right] = \left[\text{Present Value of Inflows of Uniform Series}\right] + \left[\text{Present Value of Inflows of Gradient Series}\right] \tag{11}$$

or

$$\left[\text{Present Value of Inflows}\right] = \left[S_o(\Delta\dot{M})t\right](\text{pwf-i\%-}\eta) + \left[0.1S_o(\Delta\dot{M})t\right](\text{gpwf-i\%-}\eta) \tag{12}$$

where

(gpwf-i%-η) = factor to convert a gradient series to a present work

The factor to convert a gradient series to a present work, gpwf-i%-η, is related to the uniform present worth factor, pwf-i%-η, through the expression (6)

$$(\text{gpwf-i\%-}\eta) = (\text{gf-i\%-}\eta)(\text{pwf-i\%-}\eta) \tag{13}$$

where

gf-i%-η = factor to convert a gradient series to an equivalent annual series

By substituting Equations (6), (12) and (13) into Equation (5), the following relationship can be obtained

$$(\text{pwf-i\%-}\eta) = \frac{S_o(\Delta\dot{M})t - F + 0.1S_o(\Delta\dot{M})(t)(\text{gf-i\%-}\eta)}{P} \tag{14}$$

All of the quantities in Equation (14) are known except (pwf-i%-η) and (gf-i%-η). Both of the factors can be considered functions of $\underline{i}$ alone since $\underline{\eta}$ will be specified. The problem is to determine the value of $\underline{i}$ that will make the left hand side and the right hand side of Equation (14) equal. Since the expressions for (pwf-i%-η) and (gf-i%-η) in terms of $\underline{i}$ are complicated, the value of $\underline{i}$ making the two sides equal must be determined by trial and error. The value of $\underline{i}$ satisfying Equation (14) is equivalent to the Internal Rate of Return (IRR).

The economics of utilizing the Machnozzle to predry three common types of fabrics (100% woven polyester, 100% woven cotton, and 50/50 woven polyester/cotton) were investigated. The pilot-scale data, summarized in Table 12, were used in this analysis. Several assumptions were made so that the Internal Rate of Return (IRR) could be calculated. The assumptions were:

1. The cost of the Machnozzle is $250 per linear inch.
2. The widths of the Machnozzle and the fabric to be processed is 60 inches.
3. The cost of the recovery system is $10,000. If the recovery system is used, 50% of the thermal energy in the steam will be recovered.
4. The life of the Machnozzle is ten years, and the salvage value of the Machnozzle and recovery system will be zero at the end of ten years.
5. The Machnozzle is utilized 5200 hours per year.
6. The maintenance cost of the Machnozzle is $1000 per year.
7. The steam consumption of steam cans is 1.5 pounds of steam per pound of water removed.
8. The production of one pound of steam requires 1000 BTU's.
9. The boiler efficiency is 80%.

Using the pilot-scale data and the assumptions, Internal Rate of Return (IRR) was calculated for the following four prices of energy:

1. $3.00 per million BTU
2. ($3.00 + 10% per year) per million BTU

Table 12. Machnozzle Pilot-Scale Data Used in Economic Analysis

Fabric Type	ρ_f Fabric Weight (oz/yd^2)	V_f Fabric Speed (M/Min)	γ_{IN} Incoming Moisture (%)	γ_{OUT} Exiting Moisture (%)	Steam Supply Pressure (psig)	Machnozzle Steam Consumption (lb/hr-inch)	Water Removed by Machnozzle (lb/hr-inch)	E_M Steam Requirement of Machnozzle (lbs of steam/lb of water removed	$\Delta\gamma$ (lbw/lbf)
100% woven polyester	1.8	80	60.5	5.9	90	17	9.0	1.9	0.55
		60	59.0	3.9		15.5	6.8	2.3	0.55
		20	68.4	2.5		13.9	2.7	5.1	0.66
100% woven polyester	1.8	80	76.0	7.0	74	14.2	11.3	1.25	0.69
		60	73.6	5.4		14.1	8.4	1.68	0.68
		20	75.8	1.8		11.9	3.0	3.92	0.74
100% woven polyester	1.8	80	77.6	14.6	50	9.2	10.3	0.89	0.63
		60	80.6	12.7		8.3	8.4	0.97	0.68
		20	85.9	4.3		8.1	3.4	2.42	0.81
100% woven cotton	4.0	80	96.8	46.0	90	19.7	18.5	1.06	0.50
		60	97.3	43.8		20.2	14.6	1.38	0.54
		20	98.8	34.2		18.1	5.9	3.07	0.65
100% woven cotton	4.0	80	101.8	52.4	74	16.2	18.0	0.90	0.49
		60	99.0	49.1		16.2	13.6	1.19	0.59
		20	100.0	40.6		14.1	5.4	2.60	0.59
100% woven cotton	4.0	80	97.5	62.0	50	12.2	12.9	0.94	0.36
		60	99.2	59.2		10.7	10.9	0.98	0.40
		20	102.6	47.4		9.0	5.0	1.91	0.55
50/50 polyester-cotton	3.6	80	64.9	17.3	92	18.4	15.6	1.18	0.48
		60	64.6	14.9		17.9	12.2	1.47	0.50
		20	70.5	7.2		16.0	5.2	3.08	0.63
50/50 polyester-cotton	3.6	80	60.6	21.5	75	15.2	12.8	1.19	0.39
		60	62.7	18.7		15.1	10.8	1.40	0.44
		20	70.8	9.7		13.0	5.0	2.60	0.62
50/50 polyester-cotton	3.6	80	60.9	28.4	50	11.7	10.7	1.09	0.33
		60	62.3	26.3		9.5	8.8	1.08	0.36
		20	69.1	16.7		8.6	4.3	2.00	0.52

3. $6.00 per million BUT

4. ($6.00 + 10% per year) per million BTU

The results of the calculations, summarized in Table 13, show that the economic feasibility of using the Machnozzle as a predrying device depends on the cost of energy and process operating conditions. Internal Rate of Return (IRR) was very large (as high as 183%) in some cases, but extremely small in other cases. There were several conditions where the initial investment would not be recovered in the ten year period used in the analysis.

The price of energy greatly affects IRR, as would be expected. For example, when fabric speed is 80 meters per minute and the most economical steam supply pressure is used, IRR for an energy cost of $6 per million BTU is approximately twice that for an energy cost of $3 per million BTU. When the price of energy is $6 per million BTU, the IRR's for fabrics made of 100% polyester, 100% cotton, and 50/50 cotton/polyester are 98, 173, and 129%, respectively. The IRR's for the same three fabrics, but at an energy cost of $3 per million BTU are 47, 85, and 62%, respectively. The current cost of energy is approximately $3 per million BTU; however, the time the Machnozzle could be utilized in industry, the price of energy will no doubt be much higher. Thus, the IRR's calculated at $3 and $6 per million BTU can be considered as brackets for the actual IRR at plants where conditions are consistent with the assumptions discussed above.

The results of the economic calculations showed that in most cases adding 10% per year to the cost of energy increased IRR by approximately 10%. For example, when the price of energy is $6 per million BTU and none of the energy

Table 13. Results of the Economic Analysis

Fabric Type	Fabric Weight (oz/yd^2)	Steam Supply Pressure (psig)	Fabric Speed (M/MIN)	INTERNAL RATE OF RETURN (IRR) (%)							
				COST OF ENERGY PER MILLION BTU							
				$3		$3 Plus 10% Per Year		$6		$6 Plus 10% Per Year	
				Without Recovery	With Recovery	Without Recovery	With Recovery	Without Recovery	With Recovery	Without Recovery	With Recovery
100% woven polyester	1.8	90	80	*	14	*	22	*	40	*	50
			60	*	*	*	*	*	13	*	21
			20	*	*	*	*	*	*	*	*
100% woven polyester	1.8	74	80	9	41	17	51	36	89	46	98
			60	*	17	*	24	*	47	*	57
			20	*	*	*	*	*	*	*	*
100% woven polyester	1.8	50	80	41	47	51	56	92	98	102	108
			60	24	34	34	42	62	76	72	85
			20	*	*	*	*	*	*	*	*
100% woven cotton	4.0	90	80	56	80	65	90	121	164	131	174
			60	0	51	5	61	16	107	25	117
			20	*	*	*	*	*	*	*	*
100% woven cotton	4.0	74	80	77	85	87	94	162	173	172	183
			60	23	53	33	63	59	112	69	121
			20	*	*	*	*	*	*	*	*
100% woven cotton	4.0	50	80	49	58	59	68	107	121	117	131
			60	36	47	46	55	82	100	92	109
			20	*	*	*	*	*	*	*	*
50/50 woven polyester cotton	3.6	92	80	30	62	40	72	71	129	81	139
			60	*	39	*	47	*	83	*	93
			20	*	*	*	*	*	*	*	*
50/50 polyester-cotton	3.6	75	80	22	50	32	59	55	105	65	114
			60	*	35	*	43	*	77	*	87
			20	*	*	*	*	*	*	*	*
50/50 polyester-cotton	3.6	50	80	24	42	34	52	62	92	72	101
			60	18	34	28	42	51	76	61	85
			20	*	*	*	*	*	10	*	18

* For thoses cases, either investment would not be recovered in ten years or IRR is extremely small.

is recovered, the IRR for the woven 100% cotton fabric (processed using a fabric speed of 80 meters per minute and a steam supply pressure of 90 psig) is 121%. For the same conditions except that the price of energy is $6 per million BTU plus 10% per year, the IRR is 131%.

Utilization of a heat recovery system with the Machnozzle increased IRR for all the cases considered. However, the magnitude of the increase varied significantly with operating conditions. In some cases, IRR increased only a few percent, but in other cases, IRR increased significantly (as much as 58%).

In general, IRR increased with increasing fabric speed. This was expected since productivity increases linearly with fabric speed while energy consumption of the Machnozzle increases only slightly. The highest fabric speed (80 meters per minute) for which IRR was calculated corresponds closely with process speeds used in industry.

The IRR's, summarized in Table 13, indicate that the Machnozzle can be economically attractive as a fabric predrying device. As mentioned previously, the IRR's are based on pilot-scale data and the assumptions discussed above. For the IRR's in Table 13 to translate to actual commercial conditions, the plant operating conditions must be consistent with those used in this study. Many industrial operations may have squeeze rollers that express water more efficiently that those used to obtained the pilot-scale data. Consequently, if the Machnozzle is used in those plants, the steam usage of the Machnozzle in pounds of steam per pound of water removed would be higher than obtained in this study. On the other hand, many of those plants utilize steam cans that consume more steam than the hypothetical steam system (1.5 pounds of steam per pound of water removed) used as a basis for the energy consumption calculations.

The two effects tend to offset each other.

If 50% Internal Rate of Return (IRR) is the lower limit of economically feasible energy conservation investments in the textile industry, the Machnozzle is attractive for 100% cotton fabrics and 50/50 cotton/polyester blend fabrics (with heat recovery) at an energy cost of $3 per million BTU. All three types of fabrics give favorable Internal Rate of Return (IRR) at an energy cost of $3 per million BTU plus 10% per year.

III. MATHEMATICAL MODELING OF STEAM CAN DRYING

A. INTRODUCTION

Heated cans (or drums) have been utilized for at least a century for drying sheet materials and slurries. A series of steam-heated cans are often used to dry textiles, primarily due to the convenience of handling materials on these dryers. Typically, fabrics moving at speeds ranging from 50 to 100 yards per minute pass over a battery of steam cans consisting of 20 to 48 units. The cans are normally charged with steam at pressures ranging from 40 to 70 psig. Due to the low cost of energy in the past, low energy consumption has not been a consideration in the design and operation of steam can dryers. As a result, can dryers are energy inefficient in removing water from textiles. By optimizing can dryers, a large part of the annual energy requirement for drying textiles (estimated 5.6×10^6 BOE (1)) could be conserved.

Since textile can drying represents an energy-intensive, wasteful process, one of the objectives of the research reported here was to optimize steam can dryers with respect to energy consumption. The parameters involved in can drying are numerous. Therefore a totally experimental approach to optimization would require extensive experimental testing. Since textile machines are far too expensive to operate for extensive experimentation, the approach to optimize steam can dryers has been to develop a mathematical model of the can drying process than can predict the rate of energy consumption and the corresponding drying rate for various system parameters.

B. BRIEF REVIEW OF STATE-OF-THE-ART IN CAN DRYING

A survey of the literature to determine the state-of-the-art in can drying reveals that almost nothing has been done in the textile area towards the under-

standing of can drying. However, several investigations pertaining to the can drying of paper have been conducted. Most of the earlier models used to describe paper drying have been based on a heat conduction model developed by Nissan (7,8,9). Nissan's model, however, does not include a description of mass transfer occurring within the sheet, and requires simultaneous measurement of dryer and sheeting parameters.

A number of papers dicussing the transport phenomena in porous media have been published. Due to the complex phenomena that can occur during drying of porous media, a single commonly accepted model has not emerged.

Some of the earlier drying models are based on non-isothermal mass transfer processes assuming a single dominant mechanicsm for moisture distribution. In these models, moisture is assumed to migrate by either liquid diffusion or capillarity. Taking into account simultaneous heat and mass transfer, Henry (10) proposed the vaporization-condensation theory with the basic assumption that moisture migrates entirely in the vapor phase. In most cases, these models were too simplistic and could not adequately predict drying rates (11).

The mathematical model proposed by Lyons et al (12), while incorporating both heat and mass transfer, requires that values of porosity, pore diameter, and sticking coefficient be specified.

In the last few years, more complicated models (13,14,15,16) have been developed by using mechanistic reasoning and irreversible thermodynamics. The major difference in the models has been the choice of the dominant driving forces.

The mathematical model presented by Hartley and Richards (17) assumes that liquid flux is a function of moisture content only. The effects of moisture concentration and temperature on liquid flux are important, but neglected by the model.

Fortes and Okos (11) have formulated a drying model by combining mechanistic reasoning with irreversible thermodynamics. Their model assumes that both liquid and vapor fluxes can be expressed in terms of the same driving forces, in particular, temperature and equilibrium relative humidity gradients. The model appears to be based on good assumptions and incorporates most of the accepted features of recent models.

A commonly accepted theory in the contact drying of fibrous materials is that drying begins in a short preheating period in which both the temperatures of the material and the drying rate increase, until they attain some steady state values. This is followed by a constant-rate-of-drying period characterized by vaporization from a surface saturated with free water. As drying proceeds a critical moisture content is reached when the free water concentration at the surface drops to zero and the transition to the falling-rate period of drying begins. Liquid water does not migrate to the surfaces as fast as it evaporates from the surface, and the zone of vaporization recedes into the interior leaving a dry outer layer. In this region the moisture content of the fabric is obtained from the relative humidity - desorption curve.

The effective thermal conductivity decreases as the dry layer of fabric increases, and as this layer increases, temperatures in the fabric decrease. The flows of heat and water vapor from the hot surface to the plane of minimum temperature in the fabric are concurrent and parallel (18).

C. MATHEMATICAL MODEL

1. Moisture Migration Mechanism

A modified form of Dacry's Law was used to describe the rate of liquid water flow through the fabric. The liquid flux is related to relative humidity, temperature, and their gradients. Under unsaturated conditions liquid moisture movement is negligible.

The moisture moves in the vapor phase by diffusion. The driving force for the diffusion is a vapor pressure gradient. Fick's first law was utilized to relate vapor flux to relative humidity, temperature, and their gradients.

When these relationships for the moisture fluxes were used in writing energy and mass balances, a set of equations describing the general macroscopic phenomena occurring during drying was obtained. The equations describe the temperature and moisture variations within the sheet.

In conjunction with the moisture movement mechanisms, the widely accepted evaporation-diffusion-condensation theory explaining moisture movement within a drying sheet was included in the model. According to the evaporation-diffusion-condensation theory, water flows from an internal region of maximum moisture content toward the surfaces. Water moving through the fabric to the hot can surface is vaporized. The vapor formed in the vicinity of the hot surface diffuses back through the fabric towards the open surface. As the vapor moves back through the fabric, partial condensation can occur because of the decreasing temperature. Thus an evaporation-diffusion-condensation process is partially responsible for heat transfer as well as mass transfer in the fabric.

2. Assumptions

In deriving the set of equations describing the phenomena occurring in drying fabric sheet, several assumptions were made. The major assumptions were:

(1) The web is composed of a network of fibrous materials randomly oriented and containing liquid water, water vapor, and air in the structure voids.

(2) The fibrous structure is macroscopically uniform and isotropic, i.e., the system is taken as a continuum.

(3) Moisture migration takes place in both the liquid and vapor phases. A modified form of Darcy's law is used to relate the liquid flux to relative humidity, temperature, and their gradients.

(4) The temperatures and vapor pressures of the liquid and vapor phases are in equilibrium.

(5) The vapor pressure in the voids is equal to the product of the saturation vapor pressure for pure water at the corresponding temperature and the relative humidity.

(6) Relative humidity is a function of moisture content and temperature.

(7) Variations in the y-direction (width direction) are negligible.

(8) Mass transfer and conductive heat transfer are appreciable only in the x-direction (perpendicular to the fabric sheet).

(9) Radiative heat transfer is negligible.

(10) Shrinkage and mechanical deformations are negligible.

(11) Void fraction is constant and uniform through sheet.

(12) Densities of fiber and water are constant.

(13) No chemical reactions are assumed to occur.

(14) Air and steam are treated as ideal gases.

3. Development of Mathematical Model

Development of the mathematical model describing the can drying process was divided into three tasks:

Task 1: Writing the governing equations describing the heat and mass transfer mechanisms in the process.

Task 2: Writing the initial and boundary conditions.

Task 3: Solving the governing equations consistent with the initial and boundary conditions.

Brief descriptions of these three tasks follows:

(a) Task 1

The equations governing the heat transfer through the metal shell of the can dryer and the heat and mass transfer in the fabric sheet were written. The equations were obtained by writing energy and mass balances for the two stationary control volumes shown in Figure 20.

One of the control volumes is located in space through which the can shell rotates. Since only conductive heat-transfer occurs in the shell, the only differential equation needed to describe the temperature variation through the shell is an energy balance equation.

The other control volume is located in space through which the sheeting material flows. The phenomena occuring in this control volume are much more complex since a three phase system (gases (air and water vapor), liquid water, and solid (fibers)) exits there. Several heat-transfer mechanisms operate simultaneously in the drying fabric. The mechanisms include: conduction, convection radiation, and evaporation-diffusion-condensation. As a result, six differential equations are needed to describe the heat and mass transfer occurring in the sheet:

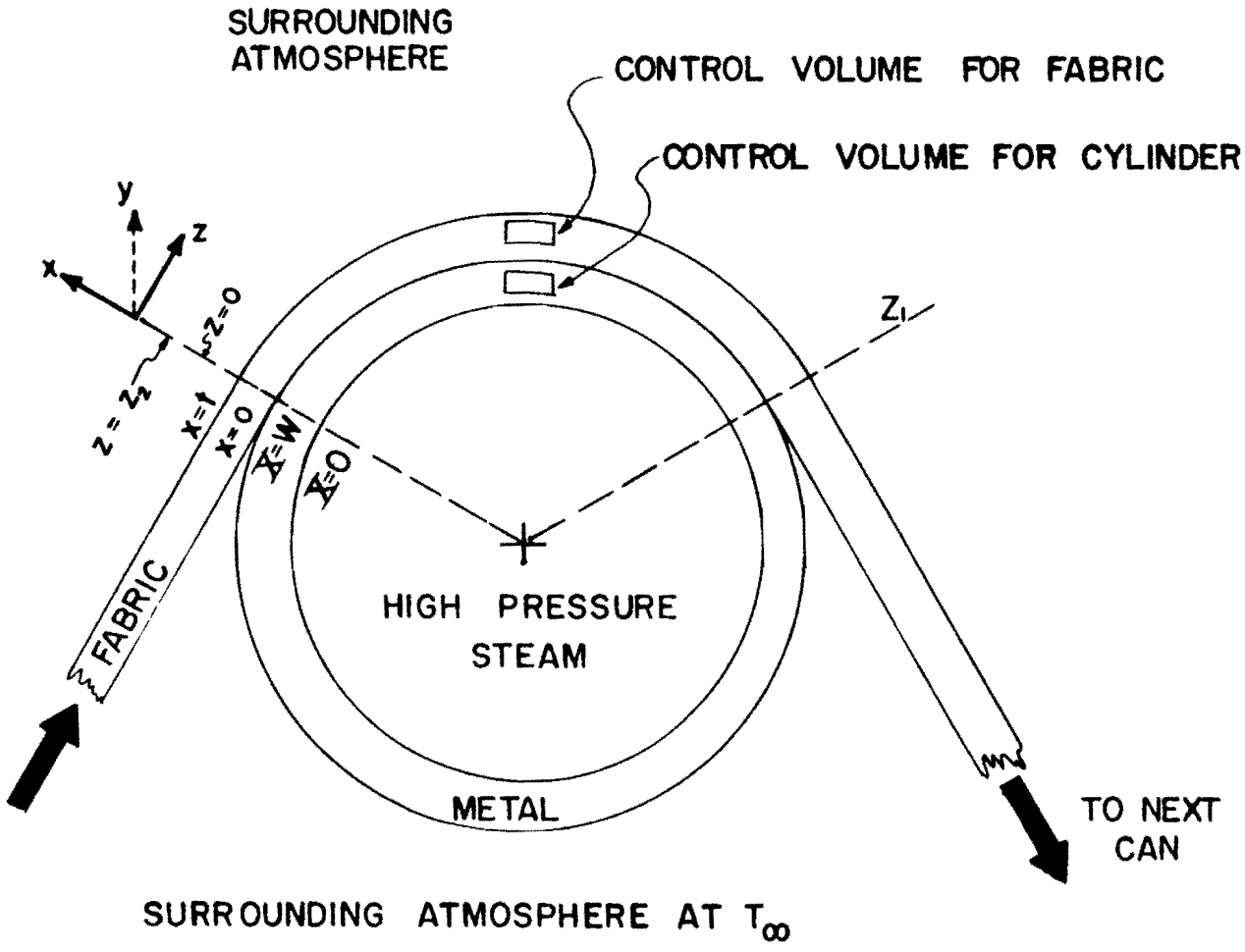

Figure 20. Schematic Of Can Dryer Showing Control Volumes Used In Deriving Governing Equations

(1) An overall energy balance

(2) Mass balance on air

(3) Mass balance on water vaor

(4) Mass balance on liquid water

(5) Relationship describing movement of liquid water in fabric

(6) Relationship for air-water vapor diffusion in a porous medium (fabric)

The equations are presented in detail in Appendix 2.

(b) Task 2

Solving the governing equations requires initial and boundary conditions for the can shell and the fabric. These conditions are presented in detail in Appendix 2.

(c) Task 3

The governing equations are nonlinear partial differential equations with second order terms, therefore, exact closed form solutions would be extremely difficult to obtain. Thus a numerical scheme was used to solve the equations. The details of the numerical scheme are discussed in Appendix 3.

D. COMPUTATIONAL RESULTS AND DISCUSSION

A lack of experimental data in the drying of fabrics precluded the possibility of any comparison between theory and experiment. However, some experimental data were available on the drying of paper. The experimental results of McCready (19) and Han and Ulmanen (20) were selected for comparison with the predictions of the theoretical model. McCready's data

pertain to the rates of drying of pulp of varying thickness. Han and Ulmanen measured moisture, temperature, and caliper data in the drying of a thick paper sheet at specific points across the thickness of the sheet.

The results of the numerical solution of the reduced and transformed non-dimensional governing equations are plotted in Figures 21 and 22. Neither McCready's nor Han and Ulmanen's data (19,20), independently, contain all the information required for the computer solution. This includes critical parameters such as heat and mass transfer coefficients, and diffusion coefficients. Therefore, only trends are compared. The temperature-time and moisture content-time profiles show similar trends to those of the experiments.

To study the effect of the sensitivity of the air-vapor diffusion coefficient, the equations were solved first using a diffusion coefficient with a value corresponding to the free stream, second with a value one-half of the previous value, and finally with a value one-tenth of the initial value. The sensitivity of the binary diffusion coefficient is clearly reflected in the plots.

Moisture Regain at the Free Surface

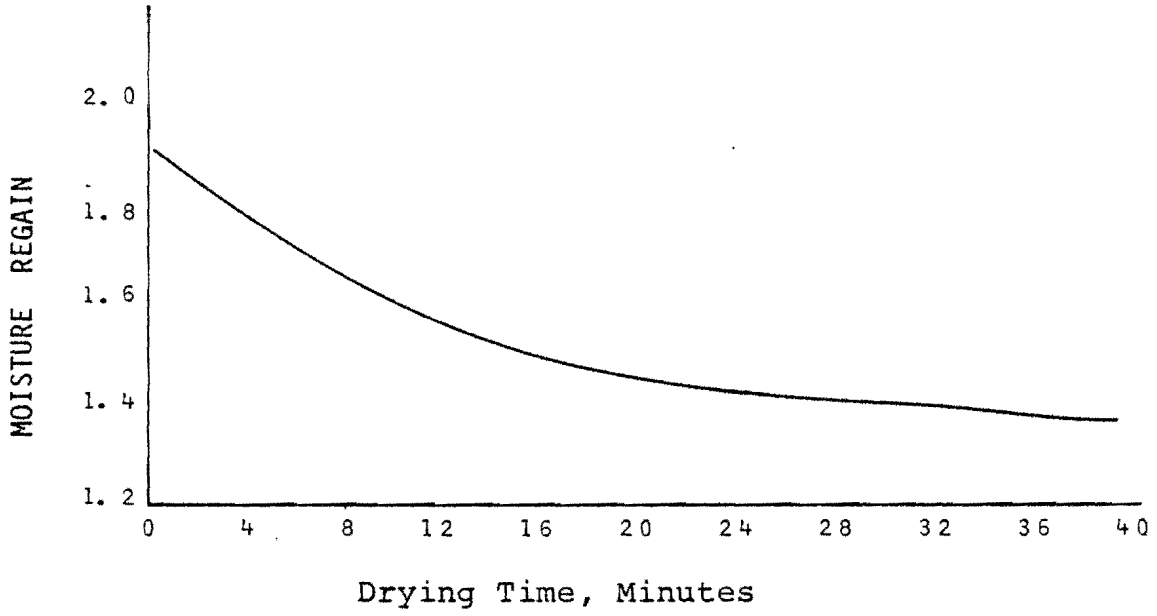

Moisture Regain-Drying Time Profile [18]

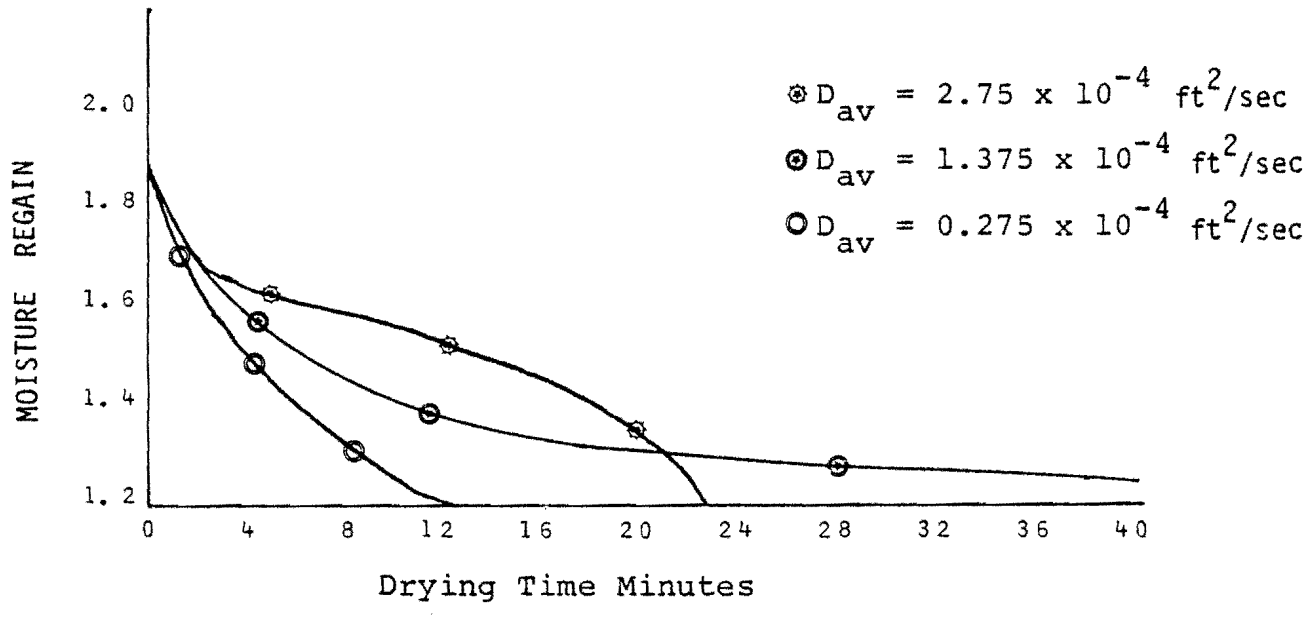

Figure 21. Comparison of Moisture Regain-Time Profiles

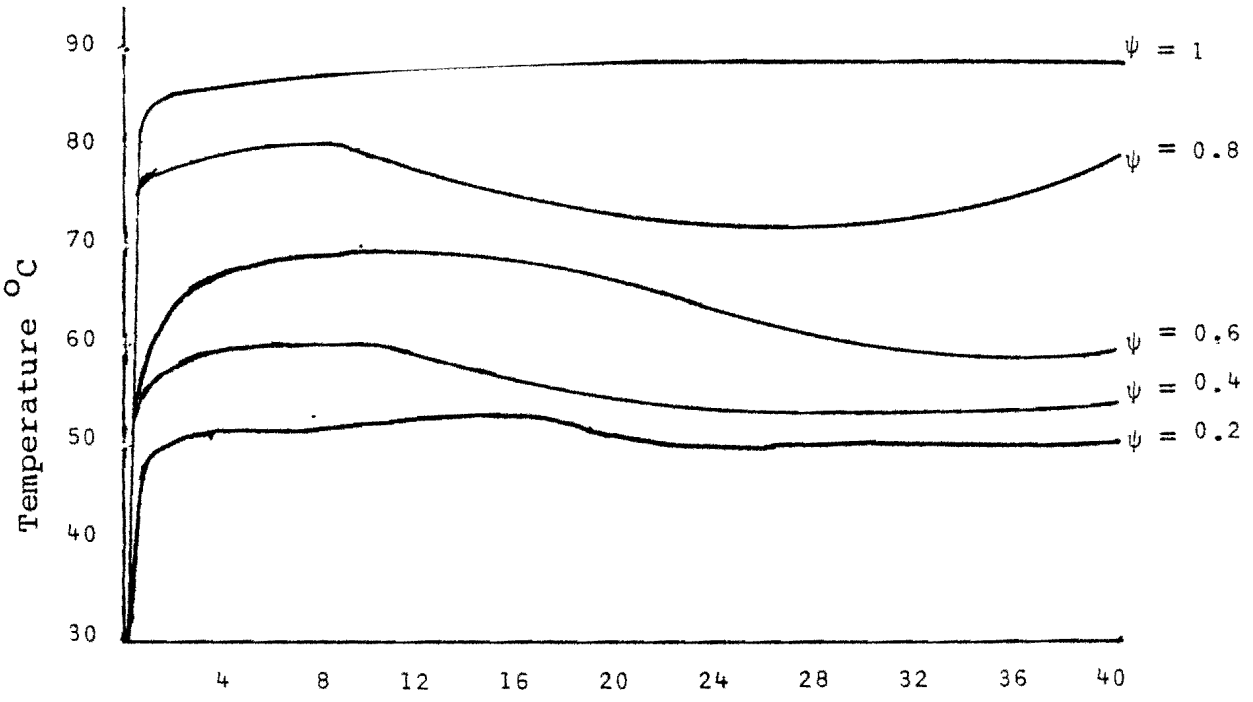

Temperature-Time Profile: (Han and Ulmanen [18])

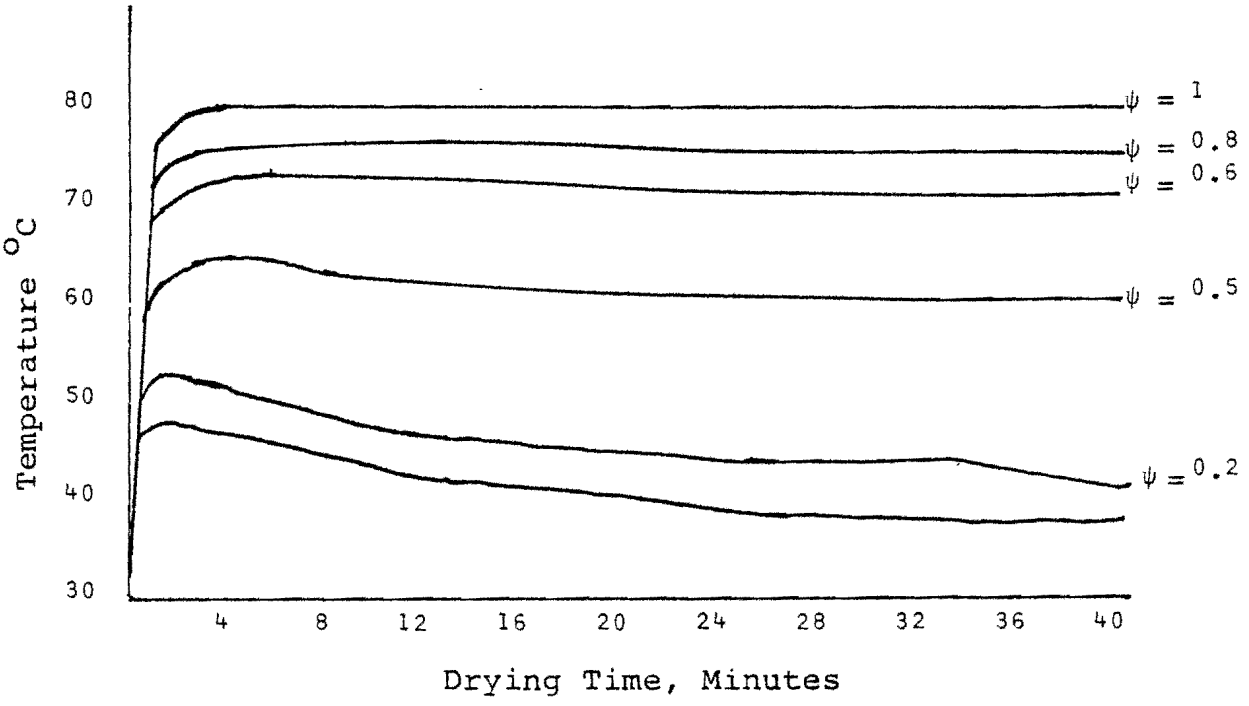

Figure 22. Comparison of Temperature Profiles

IV. DISSEMINATION OF RESULTS

Results from this study have been published and presented at a national technical meeting. A paper entitled, "Energy Consumption and Conservation: Textile Drying" by David Brookstein was published in American Chemical Society Symposium Series 107. A presentation "Drying of Fabrics With a Machnozzle" by W. W. Carr, W. Holcombe, and D. Brookstein was presented at the 1979 Textile Conference sponsored by the Textile Industries Division of ASME and the Textile Institute, England.

Technology developed during this project is also included in a course entitled "Energy Conservation in the Textile Industry" taught at Georgia Tech.

V. CONCLUSIONS

The results of the Machnozzle tests clearly demonstrate that the Machnozzle can significantly reduce the moisture content in fabrics. The economical feasibility of utilizing the Machnozzle as a fabric predrying device depends on th cost of energy and process operating conditions, in particular fabric speed. Internal Rate of Return (IRR) increases with fabric speed. For a fabric speed close to plant operating speeds (80 m/min) and a realistic cost of energy ($3 per million BTU plus 10% per year), the economic analysis indicates that the Machnozzle is economically attractive. All three fabrics (100% cotton, 50/50 polyester/cotton, and 100% polyester) gave Internal Rates of Return (IRR) greater than 50%. Accordingly, the Machnozzle pilot-scale research should be expanded to an in-plant demonstration to prove the technical and economic feasibility of the Machnozzle on a commercial scale.

A mathematical model describing the physical aspects of the textile can drying process has been developed to predict drying rates. The results of the numerical scheme used to solve the governing equations show similar trends to those for experimental paper drying. Many textile fabrics dried on steam cans may be considered as hydrophilic porous media, similar to paper. However, before the model can be applied to the hot surface drying of textiles, critical parameters affecting the heat transfer rates and the mass transfer rates such as the diffusion coefficient and heat and mass transfer coefficients have to be obtained. A dearth of experimental data on these parameters indicates the need for experimentation. The sensitivity of these parameters, the diffusion coefficient for instance, has been demonstrated.

Upon the availability of such data, the mathematical model can be used with some refinement, in conjunction with feedback control systems to optimize steam can drying with respect to energy consumption.

APPENDICES

APPENDIX I

Machnozzle Test Results

Fabric	Fabric Speed (M/Min)	Incoming Moisture (%)	Exiting Moisture (%)	Incoming Moisture Range (%)	Exiting Moisture Range (%)	Steam Pressure (psig)	Steam Consumption (lb/hr)	Slot Length (in)
50/50 cotton-polyester 3.6 oz/yd^2	80	67.2	29.0	65.6-69.5	27.7-30.6		140	
	60	65.5	25.1	62.2-67.9	24.2-26.8	81		8
	20	67.4	16.3	65.7-68.8	14.9-17.2		128	
50/50 cotton-polyester 3.6 oz/yd^2	100	66.2	29.8	59.7-70.1	7.3-58.3			
	80	65.4	24.3	63.4-68	7.4-37.3	94	No	
	60	65.8	20.3	60.2-71.4	15.2-23.2		Data	8
	20	46.4	20.5	22.6-72.9	13.6-28.3			
50/50 (a) cotton-polyester 3.6 oz/yd^2	80	66.9	55.8				160	
	80	67.0	55.7			94	160	8
	80	66.3	48.7				80	
50/50 (b) cotton-polyester 3.6 oz/yd^2	80	63.6	33.4				153	8
	80	64.7	25.5			94	210	16
	80	66.2	27.1	61.7-70.8	20.4-36.7		222	16
50/50 (c) cotton-polyester 3.6 oz/yd^2	80	64.5	23.9	63.2-67.5	23.3-25.4		172	
						94		16
	80	65.2	25.6	63.2-68.0	24.6-27.0		160	

(a) Wrap angle experiment - equal wrap angles

(b) Slit width experiment - using 1 mil shim

(c) Wrap angle experiment - unequal wrap angles

APPENDIX 1 (Continued)

Fabric	Fabric Speed (M/Min)	Incoming Moisture (%)	Exiting Moisture (%)	Incoming Moisture Range (%)	Exiting Moisture Range (%)	Steam Pressure (psig)	Steam Consumption (lb/hr)	Slot Length (in)
50/50 cotton-polyester 3.6 oz/yd^2	80	67.4	40.3			94	No Data	16
	80	66.5	36.8					
100% cotton 5.67 oz/yd^2	100	103.2	67.2	102.7-103.8	66.1-68.2	94	185	16
	80	103.6	69.6	101.2-105.5	64.8-86.1		175	
	60	103.0	66.8	102.1-104.7	59.4-91.7		185	
	20	102.5	45.9	100.0-105.0	43.8-48.9		170	
100% (d) cotton 5.67 oz/yd^2	80	91.8	84.7			94	-	16
		92.6	85.0					
		93.3	63.4					
100% cotton 4.0 oz/yd^2	80	96.8	46.0	94.8-100	44.8-46.9	95	-	16
	60	97.3	43.8	94.4-102.3	40.7-48.4			
	20	98.8	34.2	96.0-102.0	32.7-35.2			
100% cotton 4.0 oz/yd^2	80	101.8	52.4	95.2-121.9	50.3-55.1	75	-	16
	60	99.0	49.1	96.6-104.4	47.2-51.5			
	20	100.0	40.6	98.2-101.3	36.3-51.9			

(d) Hot water wet out test

APPENDIX 1 (Continued)

Fabric	Fabric Speed (M/Min)	Incoming Moisture (%)	Exiting Moisture (%)	Incoming Moisture Range (%)	Exiting Moisture Range (%)	Steam Pressure (psig)	Steam Consumption (lb/hr)	Slot Length (in)
100% cotton 4.0 oz/yd^2	80	97.5	62.0	97.1- 98.3	60.4-66.7	50	-	16
	60	99.2	59.2	98.2-100.9	57.9-60.2			
	20	102.6	47.4	100.6-105.4	45.1-48.8			
100% (e) cotton 4.0 oz/yd^2	80	98.5	46.8	97.7- 99.5	44.7-50.2	95	-	16
		100.8	55.2	99.1-103.2	52.1-58.7			
100% (f) cotton 4.0 oz/yd^2	80	98.3	83.5	93.5-102.2	81.6-85.7	95	-	16
		99.6	84.2	98.3-100.8	81.9-85.0			
		100.6	88.5	99.3-101.9	84.7-91.3			
100% polyester 1.8 oz/yd^2	80	60.5	5.90	57.1- 63.8	3.13-8.47	95	-	16
	60	59.0	3.86	56.9- 61.0	3.23-4.35			
	20	68.4	2.47	58.1- 75.5	1.54-1.55			
100% polyester 1.8 oz/yd^2	80	76.0	7.00	73.0- 79.0	5.56-7.84	75	-	16
	60	73.6	5.38	69.7- 86.1	3.75-6.54			
	20	75.8	1.83	72.3- 78.4	1.09-4.00			
100% polyester 1.8 oz/yd^2	80	77.6	14.55	74.6- 80.0	11.93-17.45	50	-	16
	60	80.6	12.71	77.7- 82.4	11.45-15.38			
	20	85.9	4.31	83.0- 90.5	3.25 6.92			

(e) Tension test - (high, low)

(f) Tension test - (high, medium, low)

APPENDIX 1 (Continued)

Fabric	Fabric Speed (M/Min)	Incoming Moisture (%)	Exiting Moisture (%)	Incoming Moisture Range (%)	Exiting Moisture Range (%)	Steam Pressure (psig)	Steam Consumption (lb/hr)	Slot Length (in)
50/50 cotton-polyester 3.6 oz/yd^2	80	64.9	17.3	63.4-66.5	15.7-18.5	92	-	16
	60	64.6	14.9	63.1-65.9	13.5-16.4			
	20	70.5	7.2	67.9-73.3	5.23-8.67			
50/50 cotton-polyester 3.6 oz/yd^2	80	60.6	21.5	58.5-62.8	20.8-22.5	75	-	16
	60	62.7	18.7	56.5-67.0	18.3-19.6			
	20	70.8	9.70	67.5-73.3	8.65-10.50			
50/50 cotton-polyester 3.6 oz/yd^2	80	60.9	28.4	57.1-63.6	27.8-29.7	50	-	16
	60	62.3	26.3	60.8-65.1	25.1-27.0			
	20	69.1	16.7	67.6-70.3	15.8-17.8			

APPENDIX 2

NOMENCLATURE

a = volumetric fraction of void filled with liquid

c = total molar concentration, mols/ft^3

C_p = heat capacity at constant pressure, BTU/lb/$^\circ$R

D_{av} = air-vapor binary diffusion coefficient, ft^2/sec

h = enthalpy, BTU/lb

h_H = convective heat transfer coefficient between can, of fabric and surrounding air, BTU/ft^2/sec/$^\circ$R

h_{am} = air mass transfer coefficient, lb/ft^2/sec

h_{mv} = specific latent heat of vaporization, BTU/lb

h_{sm} = vapor mass transfer coefficient, lb/ft^2/sec

H = relative humidity

k = specific permeability, ft^2

k_{AV} = air-vapor mixture thermal conductivity, BTU/ft/sec/$^\circ$R

K = thermal conductivity, BTU/ft/sec/$^\circ$R

K_{eff} = effective thermal conductivity of sheet, BTU/ft/sec/$^\circ$R

L = total thickness of fabric/pulp slab, ft

M = moisture regain

n = mass flux, lb/sec/ft^2

P = pressure, lb/ft/sec^2

Q_l = differential heat of sorption, BTU/lb

R = gas constant, $ft^2/sec^2/^oR$

t = time, sec

T = temperature, ^oR

T_{ic} = inner surface temperature of can, ^oR

T_{fab} = temperature of fabric, ^oR

T_{sat} = saturation temperature of steam in can, ^oR

u = internal energy, BTU/lb

V = velocity along the z-direction, ft/sec

x = distance along thickness of fabric, ft

x_A = mole fraction of air

x_V = mole fraction of vapor

y = distance along width of fabric, ft

z = distance along length of fabric, ft

Subscipts

a,A = air

f,F = fiber

i = general species

l = liquid

m,w = moisture or liquid water

s,v = vapor

∞ = surrounding air conditions

0 = initial conditions

Greek

α_c = thermal diffusivity of the can shell, ft^2/sec

Δx = elemental distance along thickness of fabric, ft

Δy = elemental distance along width of fabric, ft

Δz = elemental distance along length of fabric, ft

η_1 = kinematic viscoscity, ft^2/sec

η = dimensionless flux

θ = dimensionless temperature

τ = dimensionless time

ψ = dimensionless distance

ρ = density, lb/ft^3

APPENDIX 2

Governing Equations In Steam Can Drying

A schematic of the physical process to be modeled is shown in Figure 1. The equations of continuity and energy for the fabric and the can are developed by writing mass and energy balances over a control volume for the fabric, and can respectively, subject to certain assumptions.

The major assumptions in the development of the mathematical model are:

(1) The fabric sheet is consists of a network of randomly oriented fibrous material containing liquid water, water vapor, and air in the structure of the textile voids.

(2) The fibrous structure is macroscopically uniform and isotropic, i.e., the system is a continuum.

(3) Moisture migration takes place in both the liquid and vapor phases. A modified form of Darcy's law is used to relate the liquid flux to relative humidity, temperature, and their gradients. Fick's first law is used to relate vapor flux to relative humidity, temperature and their gradients.

(4) The temperatures and vapor pressures of the liquid and vapor phases are in equilibrium.

(5) The vapor pressure in the voids is equal to the

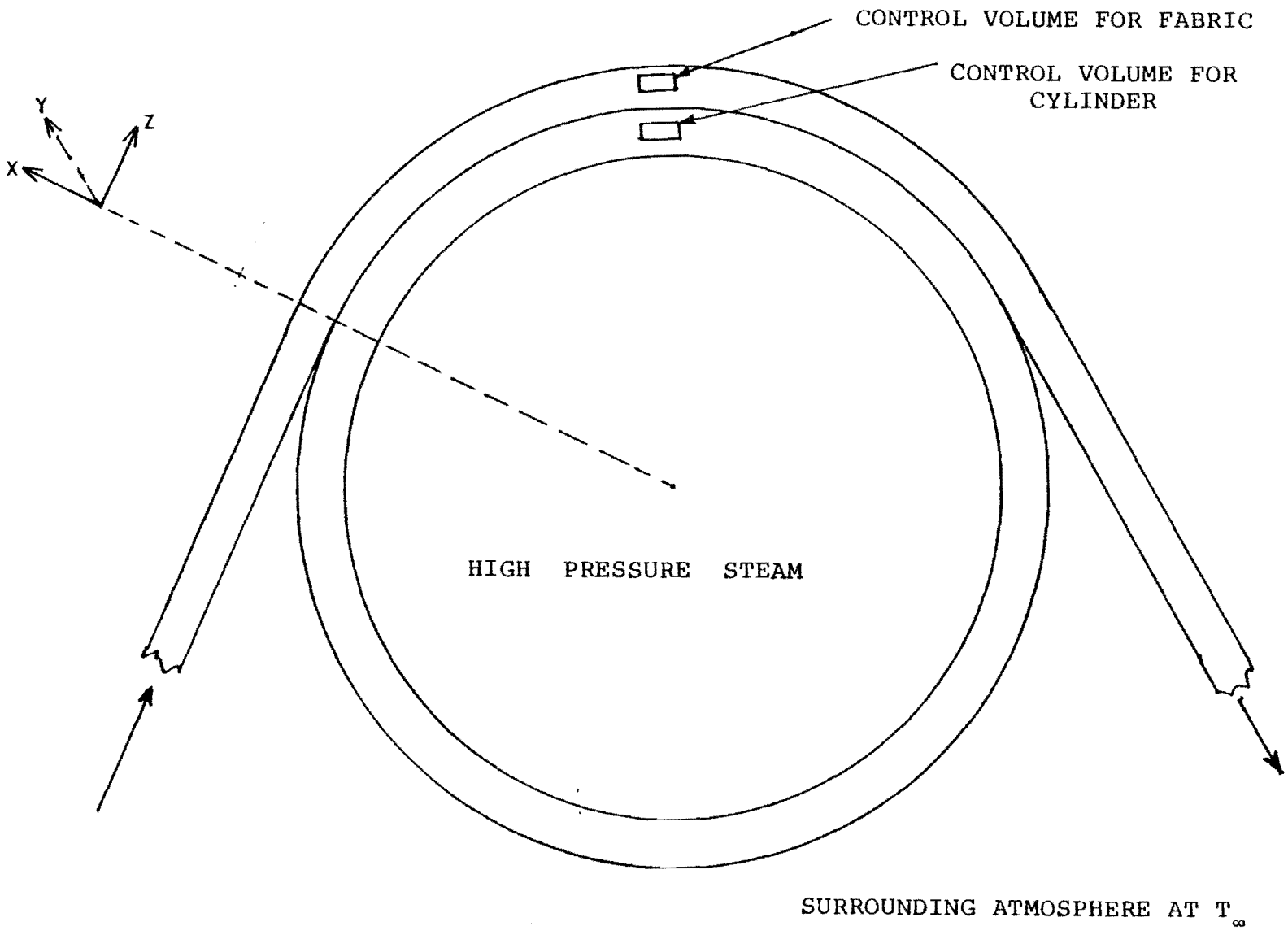

Figure 1. Schematic of Can Dryer Showing Control Volumes Used in Deriving Governing Equations

product of the saturated vapor pressure for pure water at the corresponding temperature and relative humidity.

(6) Relative humidity is a function of moisture regain.

(7) Variations across the width are negligible.

(8) Mass transfer and conductive heat transfer are appreciable only in the direction along the thickness of the fabric sheet.

(9) Radiative heat transfer is negligible.

(10) Shrinkage and mechanical deformations are negligible.

(11) Void fraction is constant and uniform throughout the sheet.

(12) Densities of fiber and water are constant.

(13) No chemical reactions occur.

(14) Air and water vapor are treated as ideal gases.

Governing Equations for Fabric

a) Mass Balance

Consider a control volume of dimensions Δx, Δy, Δz in a section of the fabric as shown in Figure 2. Based on the control volume, mass and energy balances may be written for each of the species entering and leaving the control volume.

The law of conservation of mass for any species i is written as

$$\begin{bmatrix}\text{rate of change}\\ \text{of mass of i}\\ \text{within control}\\ \text{volume}\end{bmatrix} = \begin{bmatrix}\text{rate of}\\ \text{mass of}\\ \text{i in}\end{bmatrix} - \begin{bmatrix}\text{rate of}\\ \text{mass of}\\ \text{i out}\end{bmatrix} + \begin{bmatrix}\text{rate of production}\\ \text{of mass of i within}\\ \text{control volume}\end{bmatrix} \tag{2.1}$$

If ρ_i is the mass per unit volume of species i, then the various contributions to the mass balance are:

$$\begin{matrix}\text{time rate of change}\\ \text{of mass of i within}\\ \text{control volume}\end{matrix} = \frac{\partial \rho_i}{\partial t}\,\Delta x\,\Delta y\,\Delta z \tag{2.2}$$

$$\begin{matrix}\text{input of mass of}\\ \text{i across the}\\ \text{faces at x and z}\end{matrix} = n_{i|x}\,\Delta y\,\Delta z + n_{i|z}\,\Delta x\,\Delta y \tag{2.3}$$

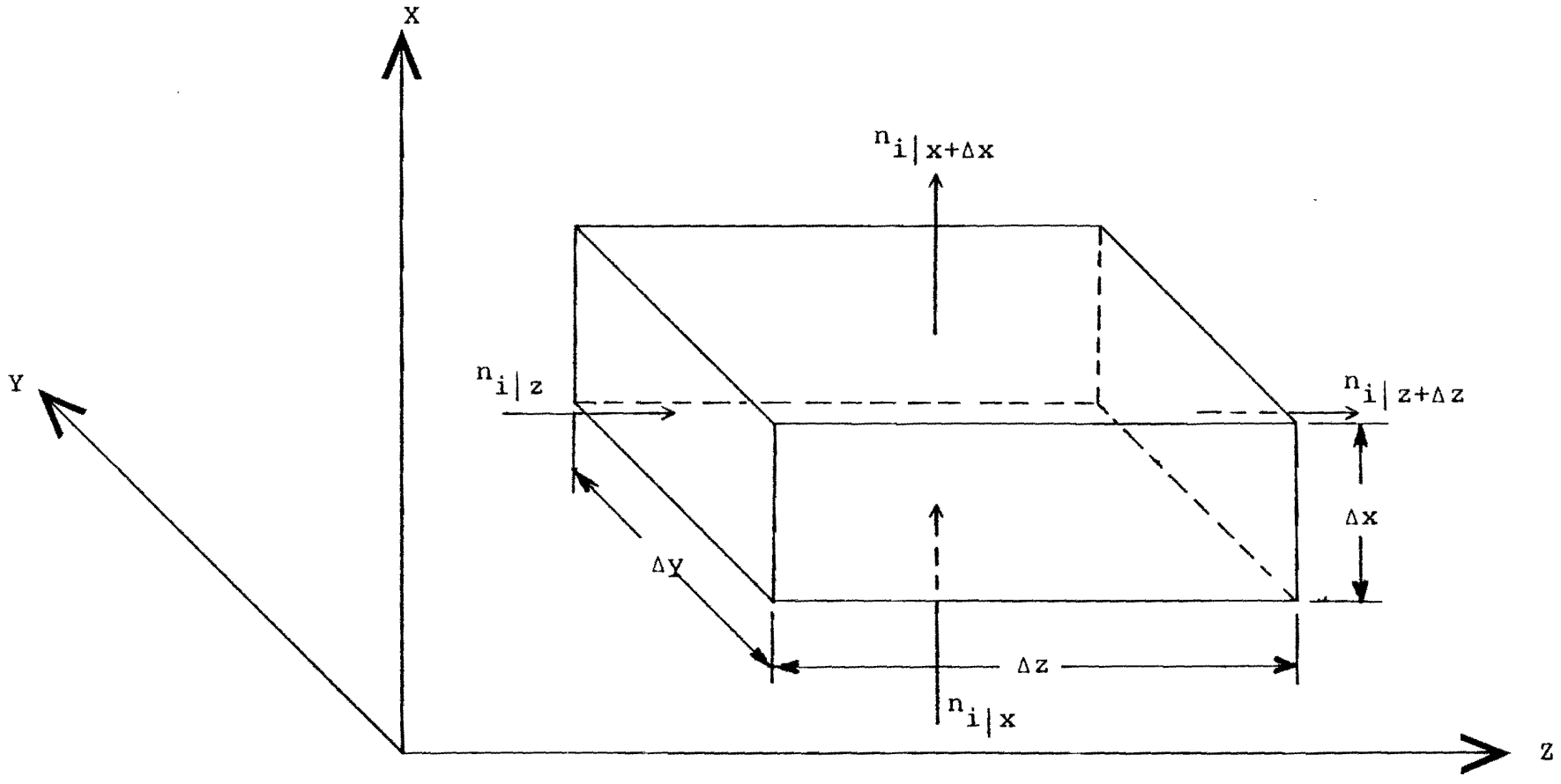

Figure 2. Control Volume Used in Deriving Mass Balance Equations

output of mass of
i across the
faces at $x + \Delta x$ and $z + \Delta z$ $= n_{i|x+\Delta x}\ \Delta y\ \Delta z + n_{i|z+\Delta z}\ \Delta x\ \Delta y$ (2.4)

rate of mass generation $= r_i\ \Delta x\ \Delta y\ \Delta z$ (2.5)

where $n_{i|x}$, $n_{i|y}$, $n_{i|z}$ are the rectangular components of the mass flux vector given by

$$n_i = \rho_i\ v_i \tag{2.6}$$

v_i is the velocity of the mass flux in the direction of the flux and r_i is the rate of mass generation per unit volume.

By assumption, the fluxes in and out of the faces at y and $y + \Delta y$ are zero.

On substitution of equations (2.2) to (2.5) in equation (2.1), dividing through by $\Delta x\ \Delta y\ \Delta z$, and taking the limit as the size of the control volume decreases to zero

$$\frac{\partial \rho_i}{\partial t} + \frac{\partial n_{i|x}}{\partial x} + \frac{\partial n_{i|z}}{\partial z} = r_i \tag{2.7}$$

Equation (2.7) is the equation of continuity of species i.

The species under consideration in this model are

(1) liquid water

(2) water vapor

(3) air

Successive application of the equation of continuity to each of the above species gives

Mass Balance for Water

$$\frac{\partial \rho_m}{\partial t} + \frac{\partial n_{m|x}}{\partial x} + \frac{\partial n_{m|z}}{\partial z} = r_m \qquad (2.8)$$

Mass Balance for Water Vapor

$$\frac{\partial \rho_s}{\partial t} + \frac{\partial n_{s|x}}{\partial x} + \frac{\partial n_{s|z}}{\partial z} = r_s \qquad (2.9)$$

Mass Balance for Air

$$\frac{\partial \rho_A}{\partial t} + \frac{\partial n_{A|x}}{\partial x} + \frac{\partial n_{A|z}}{\partial z} = r_A \qquad (2.10)$$

Since any generation of water vapor results from conversion of liquid water into vapor and vice versa,

$$r_m = -r_s \qquad (2.11)$$

and $r_A = 0$, since no air is generated.

The density terms ρ_m, ρ_s and ρ_A in equations (2.8) to (2.10) are the apparent densities of water, vapor and air. These may be related to the actual densities ρ_w, ρ_v and ρ_a by the following equations

$$\rho_m = a\ e\ \rho_w \tag{2.12}$$

$$\rho_s = (1-a)\ e\ \rho_v \tag{2.13}$$

$$\rho_A = (1-a)\ e\ \rho_a \tag{2.14}$$

where

e = volumetric void fraction

a = volumetric fraction of void filled with liquid

ρ_w = density of water

ρ_v = density of vapor

ρ_a = density of air

The mass balance equations thus become

$$\frac{\partial (ae\rho_w)}{\partial t} + \frac{\partial n_{m|x}}{\partial x} + \frac{\partial n_{m|z}}{\partial z} = r_m \tag{2.15}$$

$$\frac{\partial ((1-a)e\rho_v)}{\partial t} + \frac{\partial n_{s|x}}{\partial x} + \frac{\partial n_{s|z}}{\partial z} = -r_m \tag{2.16}$$

$$\frac{\partial((1-a)e\rho_a)}{\partial t} + \frac{\partial n_{A|x}}{\partial x} + \frac{\partial n_{A|z}}{\partial z} = 0 \qquad (2.17)$$

b) Energy Balance

The thermal energy entering the control volume at faces x, z and leaving at faces x + Δx and z + Δz is shown in Figure 3. The general macroscopic energy balance can be written as

$$\begin{bmatrix}\text{rate of change of}\\ \text{energy within}\\ \text{control volume}\end{bmatrix} = \begin{bmatrix}\text{rate of}\\ \text{energy}\\ \text{in}\end{bmatrix} - \begin{bmatrix}\text{rate of}\\ \text{energy}\\ \text{out}\end{bmatrix} + \begin{bmatrix}\text{rate of}\\ \text{energy}\\ \text{generation}\end{bmatrix} \qquad (2.18)$$

The energy in and out of the control volume at faces x and z are due to conduction and convection. No energy is assumed to enter or leave the control volume at face y.

If u_i is the energy per unit mass of the species i, then the rate of change of energy within the control volume is given by

$$\frac{\partial \rho_i u_i}{\partial t} \Delta x \, \Delta y \, \Delta z \qquad (2.19)$$

The rate of energy in is

$$q_{cond|x}\Delta y\Delta z + q_{conv|x}\Delta y\Delta z + q_{conv|z}\Delta x\Delta y \qquad (2.20)$$

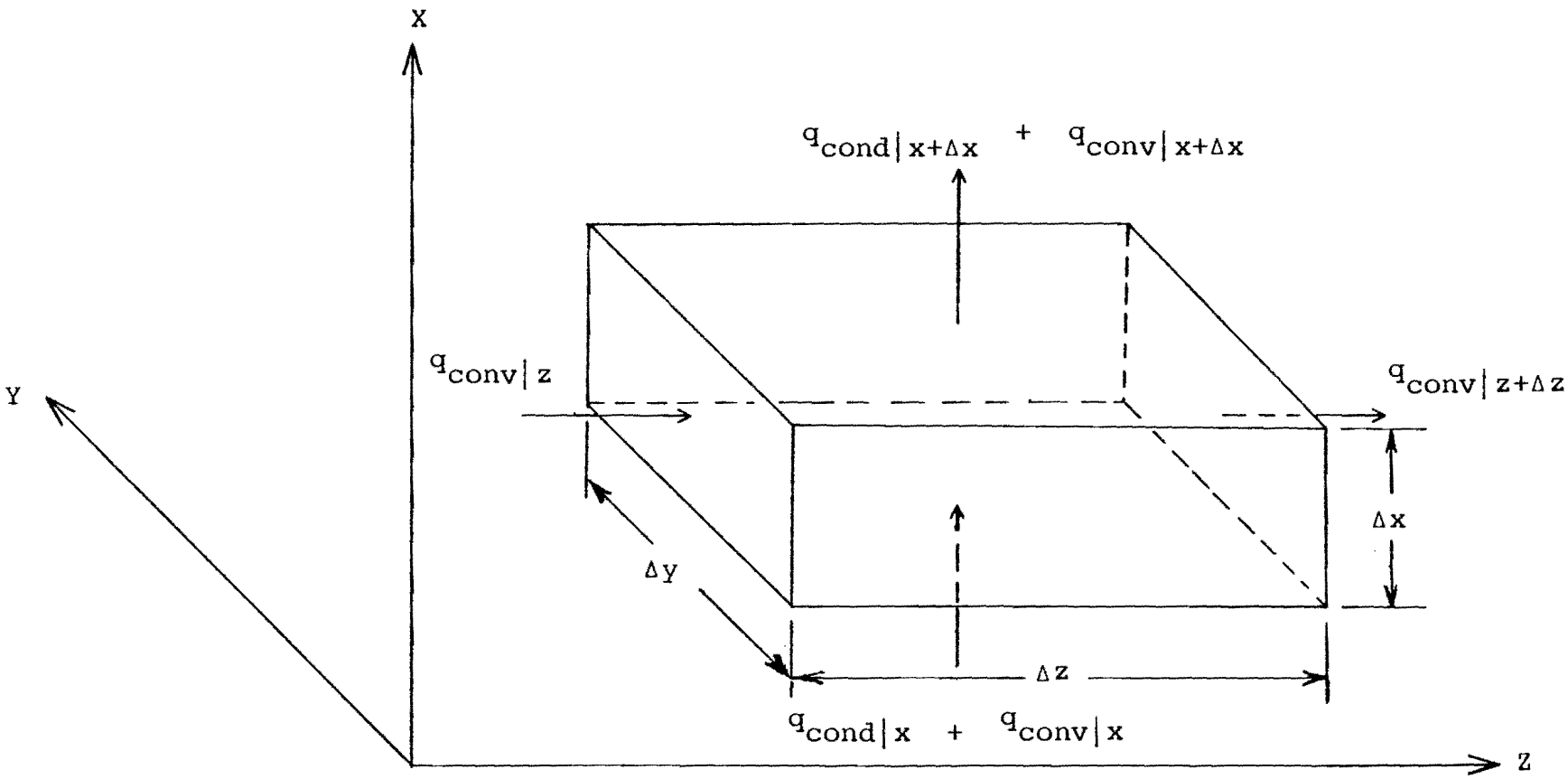

Figure 3. Control Volume Used in Deriving the Energy Equation

The rate of energy out is

$$q_{cond|x+\Delta x}\Delta y\Delta z + q_{conv|x+\Delta x}\Delta y\Delta z + q_{conv|z+\Delta z}\Delta x\Delta y \qquad (2.21)$$

where $q_{cond|x}$, $q_{cond|x+\Delta x}$ are the energy fluxes per unit area due to conduction in and out of the control volume at faces x and $x + \Delta x$. $q_{conv|x}$ and $q_{conv|z}$ are the convective fluxes per unit area into the control volume at faces x and z respectively. $q_{conv|x+\Delta x}$ and $q_{conv|z+\Delta z}$ are the convective fluxes out of the control volume at faces $x + \Delta x$ and $z + \Delta z$. By assumption the energy fluxes due to conduction at the y and z faces are zero, and the convective flux across the y and $y + \Delta y$ faces is also zero.

The rate of energy generation is zero.

Substituting equations (2.19) to (2.21) in (2.18), dividing through by $\Delta x\ \Delta y\ \Delta z$ and letting $\Delta x\ \Delta y\ \Delta z$ decrease to zero, gives

$$\frac{\partial \rho_i u_i}{\partial t} + \frac{\partial q_{cond|x}}{\partial x} + \frac{\partial q_{conv|x}}{\partial x} + \frac{\partial q_{conv|z}}{\partial z} = 0 \qquad (2.22)$$

From Fourier's law of heat conduction

$$q_{cond\ x} = -K_{eff}\frac{\partial T}{\partial x} \qquad (2.23)$$

where T is the temperature and K_{eff} is the effective thermal conductivity of the system in the control volume.

Also

$$q_{conv|x} = n_{f|x}h_f + n_{m|x}h_m + n_{s|x}h_s + n_{A|x}h_a \qquad (2.24)$$

and

$$q_{conv|z} = n_{f|z}h_f + n_{m|z}h_m + n_{s|z}h_s + n_{A|z}h_a \qquad (2.25)$$

where h_f, h_m, h_s and h_a are the enthalpies of fiber, water, vapor and air respectively. However, $n_{f|x}$ in equation (2.24) is zero since there is no movement of fiber in the x direction.

Thus

$$q_{conv|x} = n_{m|x}h_m + n_{s|x}h_s + n_{A|x}h_a \qquad (2.26)$$

Now

$$h_i = u_i + P_iV \qquad (2.27)$$

where P_i is the the pressure and V is volume.

Hence

$$\rho_i h_i = \rho_i u_i + \rho_i P_i V \qquad (2.28)$$

For an ideal gas

$$P_i V = R_i T \tag{2.29}$$

and

$$\rho_i = \frac{P_i}{R_i T} \tag{2.30}$$

from which

$$P_i V = \frac{P_i}{\rho_i} \tag{2.31}$$

Equation (2.28) may therefore be written as

$$\rho_i h_i = \rho_i u_i + P_i \tag{2.32}$$

Thus

$$\rho_A h_a = u_a h_a + P_a \tag{2.33}$$

$$\rho_s h_s = u_s h_s + P_{v0} \tag{2.34}$$

where P_{v0} is the saturated vapor pressure and P_a is the pressure due to air.

Adding equations (2.33) and (2.34) and differentiating with respect to t

$$\frac{\partial(\rho_s h_s + \rho_A h_a)}{\partial t} = \frac{\partial(u_A h_a + u_s h_s)}{\partial t} \tag{2.35}$$

since

$$P_{atm} = P_{v0} + P_a \tag{2.36}$$

and the derivative of P_{atm} with respect to t is zero. Also

$$\rho_f h_f \cong \rho_f u_f + \rho_f P_f V \tag{2.37}$$

$$\rho_m h_m \cong \rho_m u_m + \rho_m P_m V \tag{2.38}$$

where P_f and P_m are the pressures on the fiber and moisture respectively, and

$$P_f = P_m = P_{atm} \tag{2.39}$$

Adding equations (2.37) and (2.38) and differentiating with

respect to t

$$\frac{\partial(\rho_f u_f + \rho_m u_m)}{\partial t} = \frac{\partial(\rho_f h_f + \rho_m h_m)}{\partial t} \tag{2.40}$$

Combining equations (2.35) and (2.40)

$$\frac{\partial(\rho_f u_f + \rho_m u_m + \rho_s u_s + \rho_A u_A)}{\partial t} = \frac{\partial(\rho_f h_f + \rho_m h_m + \rho_s h_s + \rho_A h_a)}{\partial t} \tag{2.41}$$

Thus the energy balance may be written as

$$\frac{\partial(\rho_f h_f + \rho_m h_m + \rho_s h_s + \rho_A h_a)}{\partial t} + \frac{\partial(n_{m|x} h_m + n_{s|x} h_s + n_{A|x} h_a)}{\partial x} + \frac{\partial(n_{f|z} h_f + n_{m|z} h_m + n_{s|z} h_s + n_{A|z} h_a)}{\partial z} = \frac{\partial(K_{eff} \frac{\partial T}{\partial x})}{\partial x} \tag{2.42}$$

If $n_{f|z}$ is assumed to be constant, the derivative with respect to z vanishes.

Grouping terms, using equations (2.15) to (2.17) and simplifying:

$$\rho_f \frac{\partial h_f}{\partial t} + \rho_m \frac{\partial h_m}{\partial t} + \rho_s \frac{\partial h_s}{\partial t} + \rho_a \frac{\partial h_a}{\partial t}$$
$$+ n_{m|x} \frac{\partial h_m}{\partial x} + n_{s|x} \frac{\partial h_s}{\partial x} + n_{s|x} \frac{\partial h_a}{\partial x} + n_{f|z} \frac{\partial h_f}{\partial z}$$
$$+ n_{m|z} \frac{\partial h_m}{\partial z} + n_{s|z} \frac{\partial h_s}{\partial z} + n_{a|z} \frac{\partial h_a}{\partial z}$$
$$= \frac{\partial}{\partial x}\left(K_{eff} \frac{\partial T}{\partial x}\right) + r_m(h_s - h_m) \qquad (2.43)$$

The enthalpy h is a function of temperature T and pressure P thus

$$h = h(T,P) \qquad (2.44)$$

and

$$dh = \left(\frac{\partial h}{\partial T}\right)_P dT + \left(\frac{\partial h}{\partial P}\right)_T dP \qquad (2.45)$$

Since the derivative with respect to P is negligible,

$$dh = C_p dT \tag{2.46}$$

where h is the enthalpy and C_p is the heat capacity at constant pressure.

Therefore

$$\frac{\partial h_i}{\partial t} = C_{pi}\frac{\partial T}{\partial t} \tag{2.47}$$

$$\frac{\partial h_i}{\partial x}^{i} = C_{pi}\frac{\partial T}{\partial x} \tag{2.48}$$

$$\frac{\partial h_i}{\partial z}^{i} = C_{pi}\frac{\partial T}{\partial z} \tag{2.49}$$

The enthalpy of water in the control volume h_m is the enthalpy of water h_l minus the heat of sorption Q_l of the fibrous material the fabric is composed of. Hence

$$h_m = h_l - Q_l \tag{2.50}$$

The latent heat of vaporization is given by

$$h_{mv} = h_s - h_l \tag{2.51}$$

Substituting equations (2.47) to (2.51) in (2.43) the energy equation becomes

$$(\rho_f C_{pf} + \rho_m C_{pm} + \rho_s C_{pv} + \rho_A C_{pa})\frac{\partial T}{\partial t}$$

$$+ (n_{m|x} C_{pm} + n_{s|x} C_{pv} + n_{A|x} C_{pa})\frac{\partial T}{\partial x}$$

$$+ (n_{f|z} C_{pf} + n_{m|z} C_{pm} + n_{s|z} C_{pv} + n_{A|z} C_{pa})\frac{\partial T}{\partial z}$$

$$= \frac{\partial}{\partial x}\left(K_{eff}\frac{\partial T}{\partial x}\right) + r_m(h_{mv} + Q_l) \qquad (2.52)$$

The effective thermal conductivity of the system is taken as a function of the proportion of each constituent and moisture content in the control volume. The "resistances" to heat flow are taken to be in parallel. Hence

$$K_{eff} = (1-e)K_f + aeK_w + (1-a)e(\omega_s K_v + \omega_a K_A) \qquad (2.53)$$

where

$$\omega_a = \frac{P_a}{P_{atm}} \qquad (2.54)$$

$$\omega_s = \frac{H\ P_v}{P_{atm}} \tag{2.55}$$

$$P_{atm} = P_a + H\ P_v \tag{2.56}$$

K_f, K_w, K_v and K_A are the thermal conductivities of fiber, water, vapor, and air. P_a and P_v are the pressures at saturation due to air and vapor and H is the relative humidity.

A modified form of Darcy's law is used to describe the liquid flux $n_{m|x}$ through the fabric. The liquid flux becomes important only when then the moisture content in the fabric drops below the saturation regain of the fiber/fibers the fabric is composed of.

Darcy's equation relates the velocity of the flux (flow per unit area per unit time) to the hydrostatic pressure difference Δp, specific permeability k, thickness Δx and the kinematic viscosity of the liquid η_l.
Thus

$$v_m = - \frac{k}{\eta_l} \frac{\Delta p}{\Delta x} \tag{2.57}$$

The hydrostatic pressure difference or the water potential

is composed of both the capillary and osmotic potentials [18]. Fortes and Okos [11] have shown that the water potential p can be expressed as

$$p = R_v T(\ln H) \tag{2.58}$$

where R_v is the gas constant for vapor.
Hence

$$n_{m|x} = -\rho_m \frac{K}{\eta_1} R_v \frac{d}{dx} (T \ln H) \tag{2.59}$$

Plots of relative humidity versus regain can be found in the literature [21,22,23]. The moisture regain M is related to a - the volumetric fraction of void filled with liquid thus

$$M = \frac{ae\,\rho_w}{(1-e)\rho_F} \tag{2.60}$$

The air-vapor binary diffusion equation is given by Fick's first law

$$n_{A|x} = n_{s|x} \frac{\rho_A}{\rho_s} - \rho_s D_{av} \frac{\partial}{\partial x}\left(\frac{\rho_A}{\rho_s}\right) \tag{2.61}$$

where D_{av} is the binary air - vapor diffusion coefficient.

Governing Equation for Can

The heat transfer through the can may be described by writing an energy balance on a control volume taken in the shell of the can. The resulting equation is the Fourier Heat Conduction Equation

$$\frac{\partial T}{\partial t} = \alpha_c \frac{\partial^2 T}{\partial x^2} \qquad (2.62)$$

where α_c is the thermal diffusivity of the can shell.

INITIAL AND BOUNDARY CONDITIONS

The initial and thermal boundary conditions required for the solution of the governing equations are presented in this section.

Thermal Boundary Conditions for the Can Shell

The inner surface temperature T_{ic} of the can is assumed to be equal to the temperature at the saturation pressure of the steam in the can. Hence

$$T_{ic|t} = T_{sat} \quad \text{for all } t. \tag{2.63}$$

There are two boundary conditions for the outer surface of the can because the fabric is in contact with only a part of the can during its cycle of rotation (see Fig. 1).

The rate at which heat is conducted from the can surface is equal to the rate at which heat is convected away by the surrounding air. Therefore, the boundary condition for the region where no fabric is in contact with the can is

$$q_{sc} = h_H (T_{sc}-T_\infty) \tag{2.64}$$

The heat conducted out of the can shell is equal to the heat flow into the fabric. Hence the boundary condition for the region where the fabric is contact with the can is

$$T_{sc} = T_{fab} \tag{2.65}$$

Boundary Conditions at the Can-Fabic Interface

The surface of the can is impervious to flow and therefore, the fluxes due to liquid water, water vapor, and air are zero. Hence

$$n_{m|x} = 0 \tag{2.66}$$

$$n_{s|x} = 0 \tag{2.67}$$

$$n_{A|x} = 0 \tag{2.68}$$

Boundary Conditions at the Free Surface of Fabric

The net rate of energy leaving the fabric sheet at the free surface due to conduction and mass fluxes of vapor and air is equal to the rate at which energy is convected away from the surrounding environment, thus

$$q_{|x=L} = h_H \, (T-T_\infty)_{|x=L} \tag{2.69}$$

and the heat transferred out of the surface is

$$q_{|x=L} = \left(-K_{eff} \frac{\partial T}{\partial x} - n_s h_s - n_A h_a\right)_{|x=L} \tag{2.70}$$

The mass transfer boundary conditions at the free surface are

$$n_{s|x=L} = h_{sm} \left(P_{v0} - HP_{v\infty}\right) \tag{2.71}$$

and

$$n_{A|x=L} = h_{am} \left(P_a - P_{a\infty}\right) \tag{2.72}$$

Also

$$n_{m|x=L} = 0 \tag{2.73}$$

since no liquid water flows out of the surface.

Initial Conditions

The initial conditions of the temperature and moisture profiles in the fabric sheet just before the latter contacts the can are assumed to be uniform across the fabric sheet.

The initial conditions are

$$T_{|x,t=0} = T_0 \tag{2.74}$$

$$a_{|x,t=0} = a_0 \tag{2.75}$$

As each succeeding can is reached the roles of the surfaces of the fabric sheet are reversed. However, the boundary conditions specified for the preceeding can are easily modified to apply to the succeeding can. The temperature and moisture profiles in the fabric sheet just before contacting the succeeding can are the initial conditions for that can.

APPENDIX 3

NOMENCLATURE

a = volumetric fraction of void filled with liquid

c = total molar concentration, mols/ft^3

C_p = heat capacity at constant pressure, BTU/lb/$^\circ$R

D_{av} = air-vapor binary diffusion coefficient, ft^2/sec

h = enthalpy, BTU/lb

h_H = convective heat transfer coefficient between can, of fabric and surrounding air, BTU/ft^2/sec/$^\circ$R

h_{am} = air mass transfer coefficient, lb/ft^2/sec

h_{mv} = specific latent heat of vaporization, BTU/lb

h_{sm} = vapor mass transfer coefficient, lb/ft^2/sec

H = relative humidity

k = specific permeability, ft^2

k_{AV} = air-vapor mixture thermal conductivity, BTU/ft/sec/$^\circ$R

K = thermal conductivity, BTU/ft/sec/$^\circ$R

K_{eff} = effective thermal conductivity of sheet, BTU/ft/sec/$^\circ$R

L = total thickness of fabric/pulp slab, ft

M = moisture regain

n = mass flux, lb/sec/ft^2

P = pressure, lb/ft/sec^2

Q_1 = differential heat of sorption, BTU/lb

R = gas constant, $ft^2/sec^2/^oR$

t = time, sec

T = temperature, ^oR

T_{ic} = inner surface temperature of can, ^oR

T_{fab} = temperature of fabric, ^oR

T_{sat} = saturation temperature of steam in can, ^oR

u = internal energy, BTU/lb

V = velocity along the z-direction, ft/sec

x = distance along thickness of fabric, ft

x_A = mole fraction of air

x_V = mole fraction of vapor

y = distance along width of fabric, ft

z = distance along length of fabric, ft

Subscipts

a,A = air

f,F = fiber

i = general species

l = liquid

m,w = moisture or liquid water

s,v = vapor

∞ = surrounding air conditions

0 = initial conditions

Greek

α_c = thermal diffusivity of the can shell, ft^2/sec

Δx = elemental distance along thickness of fabric, ft

Δy = elemental distance along width of fabric, ft

Δz = elemental distance along length of fabric, ft

η_1 = kinematic viscoscity, ft^2/sec

η = dimensionless flux

θ = dimensionless temperature

τ = dimensionless time

ψ = dimensionless distance

ρ = density, lb/ft^3

APPENDIX 3

Numerical Scheme

The governing equations are quasi-linear parabolic differential equations with two partial derivatives in space and one in time. In their existing form the equations are very complex and do not lend to an easy solution.

A lack of experimental data in the drying of fabrics makes comparison between theory and experiment extremely difficult. A comparison is made, therefore, with experimental results pertaining to the drying of paper; in particular, with the work of McCready [19] and Han and Ulmanen [20]. McCready's data pertains to the rate of drying of pulp slabs of various thicknesses. Han and Ulmanen measured moisture, temperature and caliper data in the drying of a thick paper sheet, at specific points across its thickness.

The numerical scheme is written for steady-state conditions. Since the governing equations are written from an Eulerian point of view, the derivatives with respect to time at steady-state are zero. However, time measured from the instant the fabric first contacts the can is an important parameter, and readily identifiable in can drying.

A transformation is made therefore, from the z - coordinate to the t - coordinate. The resulting equations now contain one space and one time derivative. This corresponds to the Lagrangian point of view.

The transformed equations are:

Mass Balance for Water

$$\frac{\partial \rho_m}{\partial t} + \frac{\partial n_{m|x}}{\partial x} = r_m \qquad (3.1)$$

Mass Balance for Vapor

$$\frac{\partial \rho_s}{\partial t} + \frac{\partial n_{s|x}}{\partial x} = -r_m \qquad (3.2)$$

Mass Balance for Air

$$\frac{\partial \rho_A}{\partial t} + \frac{\partial n_{A|x}}{\partial x} = \emptyset \qquad (3.3)$$

Energy Balance

$$(\rho_f C_{pf} + \rho_m C_{pm} + \rho_s C_{pv} + \rho_A C_{pA})\frac{\partial T}{\partial t} + (n_{m|x} C_{pm} + n_{s|x} C_{pv} + n_{A|x} C_{pA})\frac{\partial T}{\partial x} = \frac{\partial}{\partial x}(K_{eff}\frac{\partial T}{\partial x}) + r_m(h_{mv} + Q_1) \quad (3.4)$$

Binary Diffusion of Air-Vapor

$$n_{A|x} = n_{s|x}\frac{\rho_A}{\rho_s} - \rho_s D_{av}\frac{\partial}{\partial x}\left(\frac{\rho_A}{\rho_s}\right) \quad (3.5)$$

Moisture Diffusion

$$n_{m|x} = -\rho_m \frac{k}{\eta_1} R_v \frac{\partial}{\partial x}(T \ln H) \quad (3.6)$$

The nature of the one-dimensional equations at first prompted the use of the Runge-Kutta numerical integration technique. A solution for the initial-value problem was first sought. For this purpose the partial differential equations were reduced to ordinary differential equations with derivates with respect to x, and the derivatives with respect to time were substituted with estimates obtained from Han and Ulmanen's data. The governing equations were

integrated along the x-axis after the the initial values of a, T, $n_{m|x}$, $n_{s|x}$, and $n_{A|x}$ had been specified at the hot surface, together with the estimates of the derivatives of a and T with respect to time t, at fixed points across the thickness. The fibrous material of the fabric sheet was assumed to be all-cotton, and the surface temperature of the can, constant.

A Newton-Raphson iterative scheme was utilized in conjunction with the Runge-Kutta method to improve the values of the initial estimates of the time derivatives $\frac{\partial T}{\partial x}$ and $\frac{\partial a}{\partial x}$.

The solution failed to converge due to mathematical instability. Therefore, the Runge-Kutta approach was abandoned in favor of a finite difference scheme to approximate the partial derivatives with respect to both x and t.

In order to apply the finite difference scheme, the equations are first non-dimensionalized. The following dimensionless quantities are defined:

dimensionless temperature $$\theta = \frac{T-T_0}{T_s-T_0} \qquad (3.7)$$

dimensionless time $$\tau = \frac{V\,t}{L} \qquad (3.8)$$

dimensionless distance $$\psi = \frac{x}{L} \qquad (3.9)$$

dimensionless flux $$\eta = \frac{n_{s|x}}{\rho_w V} \qquad (3.10)$$

The approach is to solve the governing equations from the time the fabric first contacts the hot surface. At this stage the relative humidity is unity and hence the moisture flux and the heat of sorption are zero. The relative humidity drops below unity when the regain drops to a value of about 0.29 from the initial value. The former value corresponds to the saturation regain value of cotton.

Adding equations (3.1) and (3.2), using equations (2.12) to (2.14) and rearranging

$$(1-a)e \frac{\partial \rho_v}{\partial T} \frac{\partial T}{\partial t} + e(\rho_w - \rho_v) \frac{\partial a}{\partial t} + \frac{\partial n_{s|x}}{\partial x} = 0 \qquad (3.11)$$

Upon non-dimensionalizing, equation (3.11) becomes

$$\frac{(1-a)}{(\rho_w - \rho_v)} \frac{\partial \rho_v}{\partial T} (T_s - T_0) \frac{\partial \theta}{\partial \tau} + \frac{\partial a}{\partial \tau} + \frac{\rho_w}{e(\rho_w - \rho_v)} \frac{\partial \eta}{\partial \psi} = 0 \qquad (3.12)$$

If C_{pi} is the volumetric specific heat, then

$$C_{pi} = (1-e)\rho_F C_{pf} + ae\rho_w + (1-a)e(\rho_v C_{pv} + \rho_a C_{pa}) \qquad (3.13)$$

Non-dimensionalizing equation (3.4) gives

$$\frac{\partial\theta}{\partial\tau} - \frac{e\rho_w h_{mv}}{C_{pi}(T_s-T_0)} \frac{\partial a}{\partial\tau} = K_{eff} \frac{\partial^2\theta}{\partial\psi^2}$$

$$+ (1-a)e\, D_{av} \left(\frac{\partial\rho_a}{\partial T} - \frac{\rho_a \partial\rho_v}{\rho_v \partial T}\right) C_{pa} (T_s-T_0)\left(\frac{\partial\theta}{\partial\psi}\right)^2$$

$$- n\frac{\rho_w}{C_{pi}} (C_{pv} + \frac{\rho_a}{\rho_v} C_{pa}) \qquad (3.14)$$

and the non-dimensional form of equation (3.3) is

$$\frac{\partial n_a}{\partial\psi} = \frac{\rho_a}{\rho_v} \frac{\partial a}{\partial\tau} - (1-a)e \frac{\partial\rho_a}{\partial T} (T_s-T_0) \frac{\partial\theta}{\partial\tau} \qquad (3.15)$$

The unknowns a, T, $n_{s|x}$, and $n_{a|x}$ are evaluated by solving equations (3.5) to (3.6) and (3.12) to (3.15) together with the initial and boundary conditions. Details of the initial and boundary conditions are given in Appendix 4. Some of the boundary conditions are reproduced here for convenience.

$$n_{m|x=0} = 0 \qquad (3.16)$$

$$n_{s|x=0} = 0 \qquad (3.17)$$

$$n_{A|x=0} = 0 \tag{3.18}$$

$$q_{|x=L} = h_H \, (T-T_\infty)_{|x=L} \tag{3.19}$$

$$q_{|x=L} = \left(-K_{eff} \frac{\partial T}{\partial x} - n_s h_s - n_A h_a\right)_{|x=L} \tag{3.20}$$

$$n_{s|x=L} = h_{sm} \, (P_{v0} - H \, P_{v\infty}) \tag{3.21}$$

The explicit finite difference scheme is illustrated in Figure 1. The values of a, T, $n_{s|x}$, and $n_{A|x}$ are evaluated at 10 points across the thickness of the fabric. Point 1 corresponds to the part of the fabric in contact with the can, and point/represents the free surface. The initial values of a, T and $n_{s|x}$ are specified at time t = 0, at all points. The size of the grid is selected such that the stability criterion $\Delta\tau/\Delta\psi^2 < 1/2$ is satisfied.

The computational scheme is as follows. The heat transfer coefficient is calculated from McCready's mass transfer coefficient using the Chilton-Colburn analogy:

$$h_H = \left(\frac{\rho C_p}{c}\right)_f \left(\frac{k_{AV}}{\rho D_{av} C_p}\right)_f h_{sm} \tag{3.22}$$

where ρ, C_p, and c are the density, specific heat, and

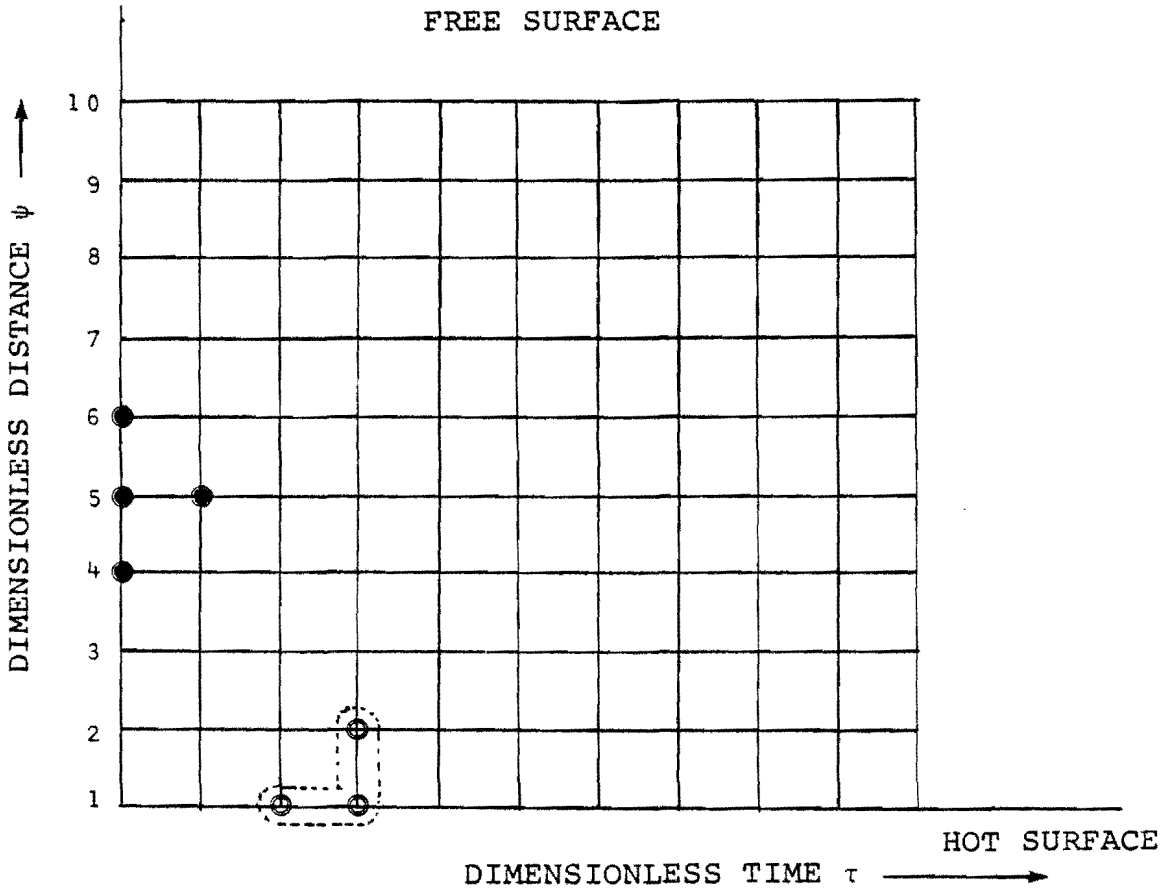

Figure 1. Finite Difference Grid showing the explicit molecule

molar concentration of the mixture of air and vapor respectively. The subscript f denotes that the properties are evaluated at the "film temperature" [24] given by

$$T_f = \frac{(T_\infty + T|_{x=L})}{2} \tag{3.23}$$

and k_{AV} is the thermal conductivity of the air-vapor mixture given by

$$(k_{AV})_f = (x_A K_A)_f + (x_V K_V)_f \tag{3.24}$$

and x_A and x_V are the mole fractions of air and vapor respectively.

Also

$$(C_p)_f = (x_A C_{pa})_f + (x_V C_{pv})_f \tag{3.35}$$

and

$$(\rho)_f = (\rho_s)_f + (\rho_A)_f \tag{3.23}$$

The values of a and T at $\tau + \Delta\tau$ and points 2 to 9 are evaluated from equations (3.12) to (3.14). The values of a and T at point 10 should simultaneously satisfy boundary

conditions (3.18) to (3.2Ø). This is accomplished by combining equations (3.18) to (3.2Ø) with equation (3.5) and using equation (3.14) at point 1Ø to solve for a and T at that point.

The value of $\underline{a}$ at the hot surface is obtained by applying equation (3.14) at the hot surface, together with the boundary conditions (3.17) and (3.18) at the hot surface. The explicit molecule for this computation is shown in dotted lines.

The values of $n_{s|x}$ and $n_{A|x}$ at points 2 to 9 are obtained from equations (3.15) and (3.5).

The entire procedure is repeated to evaluate a, T, $n_{s|x}$, and $n_{A|x}$ at $\tau + 2\Delta\tau$ ..... $\tau + n\Delta\tau$.

APPENDIX 4

Physical Properties

The expressions used in the computational scheme for the evaluation of certain physical properties are given in this Appendix.

Saturated Vapor Pressure

The saturated vapor pressure is obtained from Antoine's Equation

$$\log_{10} P_{v0} = A + \frac{B}{C + T_c}$$

where P_{v0} is the pressure in mm. of Hg., T_c is the temperature in degrees Centigrade and A, B, and C are constants:

T_c	A	B	C
< 60	8.10765	1750.286	235
≥ 60	7.96681	1668.21	228

Density of Air and Water Vapor

Since both air and water vapor are treated as ideal gases,

$$\rho_a = \frac{P_a}{R_A T}$$

and

$$\rho_v = \frac{P_{v0}}{R_v T}$$

P_{v0} is the pressure due to air and T is the temperature in degrees Rankine. R_A and R_v are the gas constants for air and vapor.

Latent heat of Vaporization of Water

$$h_{mv} = 1093.3 + 4.563095 \times 10^{-6} T_F - 1.726 \times 10^{-4} T_F^2 - T_F$$

where h_{mv} is the latent heat of vaporization of water in BTU/lb and T is the temperature in degrees Farenheit.

Thermal Conductivity

The thermal conductivities given below are for the temperature range 80 ^{0}F to 300 ^{0}F.

Water

$$K_w = R_0 T^2 + R_1 T + R_2$$

K_w is the thermal conductivity of water in BTU/hr/ft/^{0}F and

R_0 = -2.0238x10 BTU/hr/ft/ ^{0}F

R_1 = 2.93285x10 BTU/hr/ft/ ^{0}F

R_2 = 9.08334x10 BTU/hr/ft/ ^{0}F

Water Vapor

$$K_v = R_3 + R_4 T$$

K_v is the thermal conductivity of vapor in BTU/hr/ft/ ^{0}F and

R_3 = 8.29x10 BTU/hr/ft/ ^{0}F

R_4 = 2.39x10 BTU/hr/ft/ ^{0}F

Air

$$K_A = R_5 + R_6 T_F$$

K_A is the thermal conductivity of air in BTU/hr/ft/ ^{0}F and

$$R_5 = 1.347 \times 10 \quad \text{BTU/hr/ft/ } ^0\text{F}$$

$$R_6 = 1.930 \times 10 \quad \text{BTU/hr/ft/ } ^0\text{F}$$

Enthalpy of Air

$$h_a = h_{ar} + (T - T_r)$$

where T_r is a reference temperature in degrees Rankine and h_a and h_{ar} are the enthapies of air in BTU/lb at temperatures T and T_r respectively.

Heat of Sorption

The heat of sorption for cotton is obtained from the experimental results of Guthrie [25] and Rees [26].

H	Q_1
Ø.1	$W_1(\exp(W_2 H)$ x 1.8
Ø.1	(-163Ø x H + 3ØØ) x 1.8

where Q_1 is the heat of sorption and

$$W_1 = 155.13 \text{ BTU/lb}$$

$$W_2 = -1.2426$$

VII. BIBLIOGRAPHY

1. Cook, F. L., et al., "Energy Conservation in the Textile Industry," Phase I Final Technical Report DOE Project E (40-1)-5099, Georgia Institute of Technology, Atlanta, Georgia, April 1977.

2. Cook, F. L., et al., "Energy Conservation in the Textile Industry," Phase II Final Technical Report DOE Project E(40-1)-5099, Georgia Institute of Technology, Atlanta, Georgia, October 1978.

3. vander Linden, H., Wassink, J., and Theusink, C., "Andwendung der Schallstromung von Gasen und Dampfen in der Textilveredlung," Melliand Textilberichte 57 (1976), pages 53-56.

4. Theusink, C., "An Application of Sonic and Supersonic Vapor Flows in Textile Finishing," AATCC Book of Papers International Technical Conference 227, 1976.

5. Vichas, P., "Handbook of Financial Mathematics, Formulas and Tables," Prentice-Hall, Inc., Englewood Cliffs, N.J., 1979, page 126.

6. Grant, E. I., and Ireson, W. G., "Principles of Engineering Economy," The Ronald Press Company, New York, 1964.

7. Nissan, A. H., "Drying of Sheet Materials," Textile Research Journal, Vol. 38, no. 5, May 1968, pages 447-460.

8. Nissan, A. H., and Hansen, D., "Heat and Mass Transfer Transients in Cylinder Drying: Part 1. Unfelted Cylinders," A.I.Ch.E. Journal, Vol. 6, No. 4, December 1960, pages 606-611.

9. Nissan, A. H., "A Theory of Drying of Sheet Materials, By Using Heated Cylinders," Chemistry and Industry, April 7, 1956, pages 198-211.

10. Henry, P. S. H., "Diffusion in Absorbing Media," Proc. Royal Soc., 171A, 1939, pages 215-241.

11. Fortes, M., and Okos, M.R., "A Non-Equilibrium Thermodynamic Approach to Transport Phenomena in Capillary Porous Media," Proceedings of the First International Symposium on Drying, McGill University, Montreal, Canada, August 3-5, 1978, pages 100-109.

12. Lyons, D. W., Vollers, C. T., and ElNashar, A. M., "Contact Drying of a Sheet of Moist Fibrous Material," Trans. ASEM Journal of Engineering for Industry, Paper No. 79-TEX-2, Ocotober 1979.

VII. BIBLIOGRAPHY (cont'd,)

13. DeVries, D. A., and Philip, J. R., "Moisture Movement in Porous Materials Under Temperature Gradients," Trans. Am. Geophys. Union, 38(2), 1957, pages 222-232, 594.

14. DeVries, D. A., "Simultaneous Transfer of Heat and Moisture in Porous Media," Trans. Am. Geophys. Union, 39(5), 1958, pages 909-916.

15. Luikov, A. V., "Application of Irreversible Thermodynamics Methods to Investigation of Heat and Mass Transfer," Int. J. Heat and Mass Transfer, 9, 1966, pages 139-152.

16. Luikov, A. V., "Heat and Mass Transfer in Capillary-Porous Bodies," Pergammon Press, Oxford, 1966.

17. Hartley, F. T., and Richards, R. J., "Hot Surface Drying of Paper - The Development of a Diffusion Model," TAPPI, Vol. 57, No. 3, March 1974, pages 157-160.

18. Scheidegger, A. E., "Physics of Flow Through Porous Media," The MacMillan Co., New York, 1957.

19. McCready, D. W., "Drying of Pulp and Paper, III, Mechanism of Drying of Pulp Slabs on Heated Surfaces," Paper Trade Journal, TAPPI Section, September 16, 1935, pages 66-71.

20. Han, S. T., and Ulmanen Tapio, "Heat Transfer in Hot-Surface Drying of Paper," Vol. 41, No. 4, TAPPI, April 1958, pages 185-189.

21. Morton, W. E., and Hearle, J. W. S., "Physical Properties of Textile Fibres Heinemann: London, 1975.

22. Urquhart, A. R., and Williams, A. M., J. Text. Inst., 15, T559, 1924.

23. Taylor, J. B., J. Text. Inst., 43, T489, 1952.

24. Bird, R. B., Stewart, W. E. and Lightfoot, E. N., "Transport Phenomena," John Wiley and Sons, Inc., New York, 1960.

25. Guthrie, J. C., "The Integral and Differential Heats of Sorption of Water by Cellulose," J. Text. Inst., 40, 1949, T489.

26. Rees, W. H., J. Text. Inst., 39, November 1948, T351.

27. Ames, W. F., "Numerical Methods for Partial Differential Equations," Academic Press Inc., New York, 1977.

28. Mahadevan, A., "Mathematical Modeling of Steam Can Drying," Master of Science Thesis in Textile Engineering, Georgia Institute of Technology, 1980.